

Fractional calculus within the optical model used in nuclear and particle physics

Richard Herrmann

GigaHedron, Berliner Ring 80, D-63303 Dreieich, Germany

E-mail: herrmann@gigahedron.com

Abstract. The optical model is a fundamental tool to describe scattering processes in nuclear physics. The basic input is an optical model potential, which describes the refraction and absorption processes more or less schematically. Of special interest is the form of the absorption potential. With increasing energy of the incident projectile, a derivation of this potential must take into account the observed energy dependent transition from surface to volume type. The classic approach has weaknesses in this regard. We will discuss these deficiencies and will propose an alternative method based on concepts developed within the framework of fractional calculus, which allows to describe a smooth transition from surface to volume absorption in an appropriate way.

PACS numbers: 24.10.Ht, 12.39.Pn, 13.60.Fz, 13.85.Dz, 25.40.Cm, 25.40.Dn, 13.75.Cs, 21.30.Fe, 05.30.Pr, 21.30.-x

1. Introduction

In the development of physics the scattering experiments by Geiger, Marsden and Rutherford [Geiger and Marsden (1909), Rutherford (1911)] mark a twofold far-reaching highlight.

A new view on the atom emerged, overcoming Thomson's plum pudding model [Thomson (1904)] and splitting the atom into two distinct spatial areas, the outer atomic shell and the inner nucleus.

This subsequently caused a specialization of research fields of the same kind, namely from a uniform view at the atom to two at first independent research areas of atomic shell physics, which in addition covers to a large extend the study of chemical reactions and nuclear physics, which concentrates on the study of atomic nucleus itself.

Consequently these experiments mark the beginning of active research and systematic study of the properties of nuclear matter.

Besides the passive observation of nuclear properties, which started with Becquerel's [Becquerel (1896)] accidental discovery that uranium salts spontaneously emit a penetrating radiation, which he called radioactivity and in the course of time unveiled spontaneous decay phenomena (loosely sorted by emitted particle mass), like γ , β , α , cluster decay [Rose and Jones (1984)] even up to nuclear fission [Flerov and Petrzhak (1940)] now the active scattering process allowed for a detailed study of the nucleus with different projectile-target combinations within a large range of incident energies.

Motivated by Joliot and Curie's [Joliot and Curie (1934)] experiments Fermi [Fermi (1934)] performed a first systematic study for different target nuclei using slow neutrons [Fermi (1954)] from a natural beryllium source instead of α -particles as projectiles bombarding different chemical target elements. Subsequent experiments by Hahn and Strassmann [Hahn and Straßmann (1939)] were correctly interpreted as an induced fission of a nucleus by Meitner and Fritsch [Meitner and Fritsch (1939)].

The development of accelerators made it possible to realize scattering experiments with well defined projectile energies and different projectiles. While Hofstadter [Hofstatter (1956)] in Stanford used electrons to study the properties of nuclear matter, later light nuclei were used to produce trans-uranium and super-heavy elements [Oganessian *et al* (2004)].

A milestone was the acceleration of uranium beyond the Coulomb-barrier and the studies on uranium-uranium scattering at GSI in Darmstadt, which enabled to generate the strongest electromagnetic fields possible for a short time [Aleksandrov *et al* (2022)] and to study the properties of large size nuclear molecules [Reinhardt and Greiner (1977), Reinhardt *et al* (1981)].

Increasing the incident energy in heavy ion collisions allowed to investigate the properties of nuclear matter at extreme pressures and temperatures and thus to observe compression phenomena and possible phase transitions like deconfinement processes in quark-gluon-plasma [Rafelski and Müller (1982), Rafelski and Müller (1986)].

Last not least, the collision of two neutron stars [Oppenheimer and Volkoff (1939)] can be viewed as the ultimate nuclear scattering process and may be a rare event; but it generates significant signatures though which may have been detected by the LIGO experiment [Abbot *et al* (2017)].

In all these areas a vast amount of experimental scattering data for different projectile-target combinations over a large energy range has been accumulated in the last 120 years. For an interpretation and categorization of these data appropriate theoretical models had to be derived and applied.

The non relativistic optical model was developed and in the range from 1 - 200 MeV per nucleon for the incident projectile it plays an outstanding role and has proven highly successful for analysing data on elastic and inelastic scattering of nucleons, deuterons and light elements [Koning *et al* (2014)].

The basic idea behind the optical model is the interpretation of nuclear scattering using the terminology of classical optics and interpreting nuclear matter as a nebular glass body. For that purpose nuclear potentials are introduced such that the elastic and inelastic contributions of a complex scattering process are described in terms of refraction and absorption processes. At first this is a purely phenomenological ansatz which in the course of time has been motivated by a derivation of the potentials used from reasonably chosen nucleus-nucleus interactions.

In this paper, we will concentrate on absorption processes and their energy dependence described with optical model potentials. With increasing energy of the incident projectile, a derivation of this potential must consider the observed smooth transition from surface to volume absorption.

The classic approach, which is widely accepted practice for more than 60 years now cannot take this into account appropriately. But what if there was a method that could do this?!

We will first discuss the classic approach and its deficiencies and we will then propose an alternative method, which allows to describe this transition adequately.

The new approach is based on concepts developed within the framework of fractional calculus and we will demonstrate its superiority.

2. The optical model - classical approach

To begin with we will collect the necessary information on the classical derivation of optical model potentials as a basis for our criticism of the classical standard method.

The major idea behind the optical model is the representation of a nucleus by a mean field potential or optical potential $U(\vec{r}, E)$ being at least a function of space coordinates and energy of the incident particle.

The direct interaction of the incident particle with a target nucleus is considered as an interaction with the optical potential only, leading to a quantum model and the corresponding Schrödinger equation

$$\left(-\frac{\hbar^2}{2m}\Delta + U(\vec{r}, E)\right)\Psi(\vec{r}, E) = E\Psi(\vec{r}, E) \quad (1)$$

which is solved with appropriate boundary conditions leading to differential and total elastic scattering angular distributions and the reaction cross section, which is equal to the sum of cross sections for all allowed inelastic processes.

The optical potential is described by a complex quantity. Besides a real component $V(\vec{r}, E)$ which accounts for elastic scattering only it also contains an imaginary component $W(\vec{r}, E)$, which represents all inelastic processes, happening during the scattering process.

$$U(\vec{r}, E) = V(\vec{r}, E) - iW(\vec{r}, E) \quad (2)$$

In view of the optical model, these terms are interpreted as a description of refraction and absorption (note the minus sign) processes during the scattering event respectively and were first discussed as an appropriate approach for the nuclear scattering case by Ostrofsky and later Bethe [Ostrofsky *et al* (1936), Bethe (1940), Hodgson (1967)].

Since it is found experimentally that scattered nucleons are polarised even with an unpolarised incident beam, the optical model potential is extended by a spin-orbit term

$$U_{so}(\vec{r}, E) = (V_{so}(\vec{r}, E) - iW_{so}(\vec{r}, E))\vec{L} \cdot \vec{s} \quad (3)$$

where \vec{L} is the angular momentum and \vec{s} are the Pauli spin operators. From experiment, there is no evidence for a significant imaginary spin-orbit contribution, so in general the W_{so} term is ignored.

Finally, for protons as incident particles we have an additional Coulomb term $V_c(\vec{r})$.

The complete optical potential therefore is given by:

$$U_{tot}(\vec{r}, E) = V(\vec{r}, E) - iW(\vec{r}, E) + U_{so}(\vec{r}, E) + V_c(\vec{r}) \quad (4)$$

There are two types of approaches, which historically lead step by step to a reasonable form of the optical potential:

First, a phenomenological approach, using analytical functions for well depths, e.g. Woods-Saxon potentials, where the parameters are adjusted using experimental data [Woods and Saxon (1954), Becchetti and Greenlees (1969)].

Second, we have microscopic optical potentials, which are based on an effective nucleon-nucleon interaction folded with reasonable nuclear density matter distributions, where in the idealized case there is no parameter adjustment necessary [Satchler and Love (1979), Varner *et al* (1991), Woods *et al* (1982), Bauge *et al* (2001)].

A simplification, which is widely used in literature, is the restriction of the problem to spherical symmetry. The Schrödinger equation (1) can be separated in spherical coordinates and we are left with the relevant radial part with central potentials $U_{tot}(\vec{r}, E) = U_{tot}(r, E)$, with r being the distance from the scattering center and E being the energy of the incident particle.

For this case we may introduce the form factors $f(r), g(r), h(r)$, which are solely r -dependent:

$$U_{tot}(r, E) = V(E)f(r) - iW(E)g(r) + V_{so}(E)h(r) + V_c(r) \quad (5)$$

A classical choice for the central potential form factor $f(r)$ is given in close analogy to nuclear density or potential distributions used in shell model calculations or derived from mean field calculations in lowest order is the Woods-Saxon potential [Woods and Saxon (1954)]:

$$f(r) = (1 + e^{(r-R_0)/a_0})^{-1} \quad (6)$$

where R_0 is the average radius of the spherical target nucleus, which is given assuming incompressibility of nuclear matter as $R_0 = r_0 A^{1/3}$ and a_0 is a measure of the skin size of the nucleus.

The absorption form factor $g(r)$ in (5) accounts for all inelastic processes. The standard narrative for the energy dependence of this term reads as follows:

For low energies, absorption occurs mainly at the nuclear surface. Consequently for low energies the form of g is chosen as the derivative of the Woods-Saxon potential, which defines a surface contribution $g(E \approx 0) = g_s$

$$g_s(r) = -a_0 \frac{\partial}{\partial r} f(r) \quad (7)$$

where a_0 with dimension length guarantees correct potential energy units. The spin-orbit form factor $h(r)$ in (5) is then given by the Thomas-form $g(r)/r$. For higher energies absorption more and more happens throughout the nuclear volume. As a consequence being a function of energy a sliding transition from surface- to volume-absorption is observed.

Introducing an energy dependent mixing coefficient $0 \leq \omega \leq 1$ and the two potential depths W_s, W_v , with W_s denominating the strength of the surface term and W_v the strength of the volume term. The imaginary part of the central potential is therefore given as:

$$Wg(r) = \omega W_v f(r) + (1 - \omega) W_s g_s(r) \quad (8)$$

$$= \omega W_v f(r) - (1 - \omega) W_s a_0 \frac{\partial}{\partial r} f(r) \quad (9)$$

In other words: With increasing incident energy of the projectile the experimental data may be interpreted correctly assuming a smooth transition from surface to volume type absorption. Within the framework of optical potentials this behaviour is modelled by first introducing a surface potential defined as the rate of change of a given volume potential and subsequently calculating a weighted sum of these two potentials.

This procedure is common practice for more than 60 years now and has not been seriously questioned since its introduction. As an example, in figure 1 we have plotted

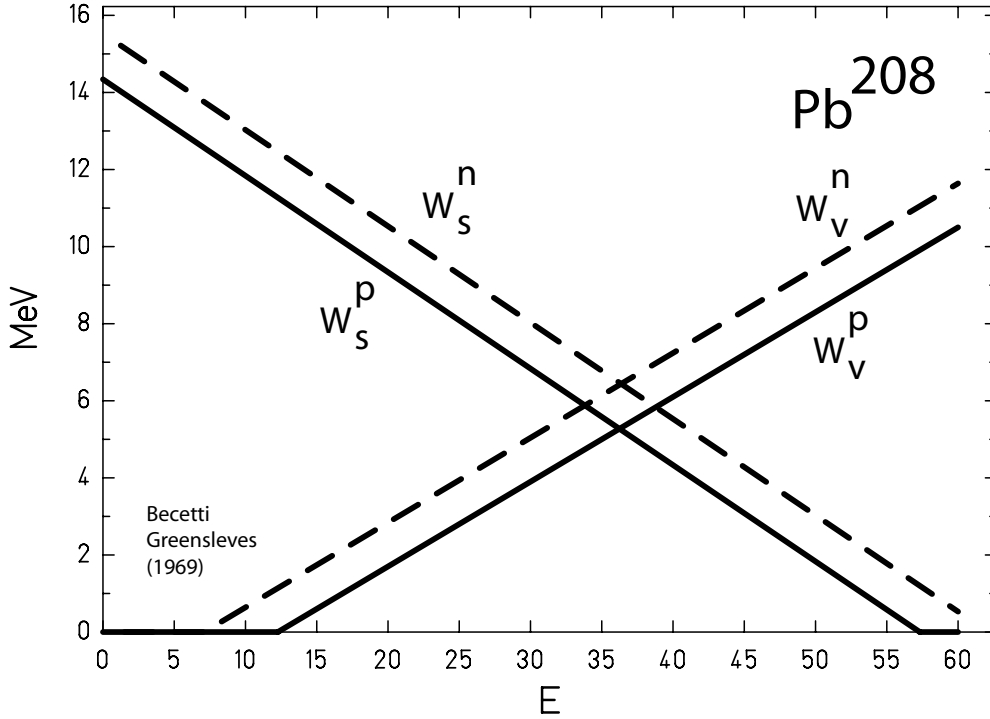


Figure 1. Energy dependence for W_v^I W_s^I for $I \in \{protons, neutrons\}$ for ^{208}Pb from [Becchetti and Greenlees (1969)]. The physically valid area is given by $E < 50$ MeV.

the energy dependence of the factors W_v and W_s (the additional factor 4 ensures comparable size range of both factors)

$$Wg(r) = (W_v - 4a_0W_s \frac{\partial}{\partial r})f(r) \quad (10)$$

for increasing energy for Pb^{208} using parameters from Becetti and Greenlees [Becchetti and Greenlees (1969)], which are valid in the region $A > 40$ and $E < 50$ MeV and are given by:

$$W_v(E) = \max \left(0, 0.22E - \begin{cases} 2.70 & \text{protons} \\ 1.56 & \text{neutrons} \end{cases} \right) \quad (11)$$

$$W_s(E) = \max \left(0, -0.25E + 12.0 \frac{N-Z}{A} + \begin{cases} 11.8 & \text{protons} \\ 13.0 & \text{neutrons} \end{cases} \right) \quad (12)$$

We conclude, that a plausible physical concept has been realized at best only pragmatically, seemingly good enough to serve as a tool in order to classify the accumulated experimental data.

A gradual transition from surface to volume potential is an essential requirement for a correct treatment of the energy dependence of the absorption term of optical model potentials. This physical fact should be correctly treated within the optical model, which has not been done so far. Neither the physical justification for this requirement nor the mathematical treatment has changed essentially through the last 60 years [Hodgson (1967), Woods *et al* (1982), Koning and Delaroche (2003)].

Already Roger Bacon in his *opus maius* pointed out, that one cause of error is the force of habit [Bacon (1267)].

So it is time for a change and a chance for a more accurate description of scattering processes within the framework of the optical model.

In the following we will propose an adequate treatment of the energy dependent absorption potential by using appropriate mathematical tools.

Our approach follows a new path to generate the progression between surface and volume absorption extending the concept of a surface definition given in terms of standard differential vector calculus.

In the following we will describe a smooth transition between first derivative (surface) potential and zeroth derivative, which means no derivative (volume) potential by applying a fractional derivative of order $\alpha \in \mathbb{R}$ to the potential such that the absorption potential becomes

$$W^\alpha = Wg(r) = W_\alpha a_o^\alpha \frac{\partial^\alpha}{\partial r^\alpha} f(r) \quad 0 \leq \alpha \leq 1, \alpha \in \mathbb{R} \quad (13)$$

For the cases $\alpha = 0$ and $\alpha = 1$ this reduces to the already known volume and surface type potential respectively, while for all intermediate cases we obtain a new fractional potential W^α , which is much closer to the physical interpretation given above than the standard approach.

We will first present the surface definition based on classical vector calculus and then we will extend this framework to the fractional case introducing an appropriate fractional derivative and will apply new fractional vector calculus methods.

3. The surface term in the optical model potentials

Nucleon density $\rho(r)$ and collective volume potential W_{vol} are related via a folding procedure of type

$$W_{\text{vol}}(r) = W_v \int_G d^3r' w(r, r') \rho(r') = W_v (w * \rho)(r) = W_v f(r) \quad (14)$$

with a weight $w(r, r')$, which models the effective short range nucleon-nucleon interaction in the collective model and the Coulomb interaction for protons respectively. It should be emphasized, that a given potential may be the result of different weight/density combinations, e.g. the weights w_C modelling a Coulomb type interaction, which may be attractive, repulsive or zero for the interacting objects with w_δ being Dirac's δ -function modelling an attractive strong contact interaction and w_Y being a Yukawa type function respectively modelling an effective soft core interaction.

$$w_C = \frac{e}{|r - r'|} \quad e \in \{+1, -1, 0\} \quad (15)$$

$$w_\delta = -\delta(|r - r'|) \quad (16)$$

$$w_Y = -e^{-\beta|r-r'|}/|r-r'| \quad \beta > 0 \quad (17)$$

and densities

$$\rho_{ws} = (1 + e^{(r-R_0)/a_0})^{-1} \quad (18)$$

$$\rho_H = H(|r - r'|) \quad (19)$$

with H being the Heavyside step function.

At first glance, it seems trivial, that a corresponding nuclear surface potential W_{surf} would be directly related to the nuclear surface S

$$\begin{aligned} W_{\text{surf}}(r) &= W_s a_0 \int_G d^3 r' w(r, r') S(r') \\ &= W_s a_0 (w * S)(r) = W_s a_0 g_s(r) \end{aligned} \quad (20)$$

with a scaling factor a_0 with dimension [fm] in order to preserve potential energy units.

But what is a nuclear surface?

An elegant general definition of a surface, which actually is as appealing as Euclid's definition of a circle, defines a surface via the spatial change of a density. In multi-dimensional space this change is calculated using the gradient operator ∇ and this is how differential calculus comes into play.

Actually there are two candidates for a useful definition of a surface:

The first one generates an absolute value:

$$S_{\text{magnitude}}(r) = |\nabla \rho(r)| = \sqrt{\nabla \rho(r) \cdot \nabla \rho(r)} \quad (21)$$

This surface definition implies isotropy of the surface generation since the gradient direction information is lost and only the magnitude remains. It measures the maximum rate of density change at a given position r and is widely used within edge detection algorithms used in image processing [Gonzales and Woods (2018)].

The second reasonable definition is oriented:

$$S_{\text{directional}}(r) = \vec{v} \cdot \nabla \rho(r) \quad (22)$$

We call this surface directional since it is based on the definition of a directional derivative, which is given by the projection of the density gradient on an arbitrary vector \vec{v} and gives the rate of density change in direction \vec{v} . Consequently in contrast to the $S_{\text{magnitude}}$ definition which always results in a positive sign for the surface, here we obtain a positive sign for the surface for increasing density and a negative sign for decreasing density.

In case of an optical model potential, the definition (22) seems appropriate, since the direction of the incident particle is important.

Therefore we obtain a possible definition for a surface potential

$$W_{\text{surf}}(r) = W_s a_0 \int_G d^3 r' w(r, r') \vec{v}' \cdot \nabla \rho(r') \quad (23)$$

where the factor a_0 has dimension length to ensure correct energy units.

In order to make our argument as clear as possible, in the following we will discuss a simplified scenario;

In the following we restrict to spherically symmetric densities $\rho(r, \phi, \theta) = \rho(r)$, restrict to collective interactions $w(|r - r'|)$ where the spatial behaviour depends on the distance only, with the volume element $\sqrt{g} = r'^2 \sin(\theta')$ and spherical surface shells setting $\vec{v}(r, \phi, \theta) = \{-1, 0, 0\}$ (23) simplifies to

$$W_{\text{Vol}}(r) = W_v \int_G \sqrt{g} dr' d\theta' d\phi' w(|r - r'|) \rho(r') \quad (24)$$

$$W_{\text{surf}}(r) = -W_s a_0 \int_G \sqrt{g} dr' d\theta' d\phi' w(|r - r'|) \frac{\partial}{\partial r'} \rho(r') \quad (25)$$

For the idealized case setting the collective nuclear interaction potential

$w(|r - r'|) = -\frac{1}{4\pi}\delta(|r - r'|)/\sqrt{g}$ we obtain the set of volume and surface potentials as

$$W_{\text{vol}}(r) = W_v f(r) \quad (26)$$

$$W_{\text{surf}}(r) = -W_s a_0 \frac{\partial}{\partial r} f(r) \quad (27)$$

Thus the problem is reduced to the one dimensional case, which suffices to clarify our viewpoint.

In order to model a gradual transition between these both limiting cases (26) and (27) we will apply methods developed within the framework of fractional calculus [Oldham and Spanier (1974), Samko *et al* (1993), Miller and Ross (1993), Podlubny (1999), Hilfer (2000), Mainardi (2010), Ortigueira (2011), Herrmann (2018)].

The basic research area of fractional calculus is to extend the conceptual framework and the corresponding definitions of a derivative operator from integer order n to arbitrary order α , where α is a real or complex value or even more complicated a complex valued function $\alpha = \alpha(r)$:

$$\frac{d^n}{dr^n} \rightarrow \frac{d^\alpha}{dr^\alpha}, \quad n \in \mathbb{N}, \alpha \in \{\mathbb{R}, \mathbb{C}\} \quad (28)$$

Several concepts coexist to realize this idea. In the following, we will first state the problem we want to solve and will then present an appropriate solution, which will much better conform with the presented physical requirements.

4. The optical model in view of fractional calculus

Extending the concept of a derivative operator to fractional order α , where α is a real number with the property $0 \leq \alpha \leq 1$, such that we obtain a smooth transition between the cases $n = 0$ and $n = 1$ allows to extend the definition of an integer gradient to a fractional gradient operator too. In cartesian coordinates we propose [Tarasov (2021)]:

$$\nabla^\alpha(x, y, z) = \left(\frac{\partial^\alpha}{\partial x^\alpha}, \frac{\partial^\alpha}{\partial y^\alpha}, \frac{\partial^\alpha}{\partial z^\alpha} \right), \quad 0 \leq \alpha \leq 1, \alpha \in \mathbb{R} \quad (29)$$

or in spherical coordinates

$$\nabla^\alpha(r, \phi, \theta) = \left(\frac{\partial^\alpha}{\partial r^\alpha}, \frac{1}{r} \frac{\partial^\alpha}{\partial \phi^\alpha}, \frac{1}{r \sin(\theta)} \frac{\partial^\alpha}{\partial \theta^\alpha} \right), \quad 0 \leq \alpha \leq 1, \alpha \in \mathbb{R} \quad (30)$$

and use this fractional gradient to define a unique fractional potential W^α in cartesian coordinates

$$W^\alpha(\vec{r}, \alpha) = W_\alpha a_0^\alpha \int_G d^3 r' w(r, r') \vec{v}' \cdot \nabla^\alpha \rho(r') \quad (31)$$

$$= W_\alpha a_0^\alpha (w * \nabla^\alpha \rho)(\vec{r}) \quad 0 \leq \alpha \leq 1, \alpha \in \mathbb{R} \quad (32)$$

where the factor a_0^α ensures correct units and the potential depth W_α is now a function of α . The limiting cases corresponding to (26) and (27) are then

$$W^\alpha(r, \alpha = 0) = W_{\text{vol}}(r) \quad (33)$$

$$W^\alpha(r, \alpha = 1) = W_{\text{surf}}(r) \quad (34)$$

and consequently the limiting cases for the potential depths

$$W_\alpha(\alpha = 0) = W_v \quad (35)$$

$$W_\alpha(\alpha = 1) = W_s \quad (36)$$

For central potentials we may switch to spherical coordinates and with $\vec{v}(r, \phi, \theta) = (-1, 0, 0)$ and are lead to the fractional extension of (27):

$$W^\alpha(r, \alpha) = W_\alpha a_0^\alpha \int_G \sqrt{g} dr' d\theta' d\phi' w(|r - r'|) \frac{\partial^\alpha}{\partial r'^\alpha} \rho(r') \quad (37)$$

$$= W_\alpha a_0^\alpha (w * \partial^\alpha \rho)(r) \quad 0 \leq \alpha \leq 1, \alpha \in \mathbb{R} \quad (38)$$

In the case of the attractive contact potential $w(|r - r'|) = -\frac{1}{4\pi} \delta(|r - r'|) / \sqrt{g}$ we explicetly obtain for the spherically symmetric fractional absorption potential W^α :

$$W^\alpha(r, \alpha) = W_\alpha a_0^\alpha \frac{\partial^\alpha}{\partial r^\alpha} \rho(r), \quad 0 \leq \alpha \leq 1, \alpha \in \mathbb{R} \quad (39)$$

With (31) for the general cartesian and (37) for the spherically symmetric case respectively we propose fractional optical model potentials for an adequate description of the energy dependence of nuclear absorption processes. In the following we will give closed form solutions for the important case of spherical Woods-Saxon type densities.

5. Derivation and applications of the spherical fractional model potential

We interpret the scattering process as a mapping from an initial to final quantum states covering the full region $\{-\infty, +\infty\}$, which for the spherically symmetric case determines the bounds for the radial component $0 \leq r < \infty$ and consequently determines the bounds for the fractional derivative definition.

For an arbitrary density $\rho(r)$ we choose a Liouville type fractional derivative [Liouville (1832)] which is defined as a sequential operation: A fractional integral with bounds $\{\infty, 0\}$ is followed by an ordinary derivative.

$$\frac{\partial^\alpha}{\partial r^\alpha} \rho(r) = \rho^{(\alpha)}(r) = \frac{\partial}{\partial r} I^{1-\alpha}(r) \rho(r) \quad (40)$$

Consequently, if we know the fractional integral I^α , we also know the fractional derivative of $\rho(r)$.

The fractional integral $I^{1-\alpha} \rho(r)$ is given by a convolution with a weakly singular kernel $w_L(h) = h^{-\alpha}$ and thus we will apply the following definition:

$$\rho^{(\alpha)}(r) = \frac{\partial}{\partial r} (w_L * \rho)(r) \quad (41)$$

$$= \frac{1}{\Gamma(1-\alpha)} \frac{\partial}{\partial r} \int_\infty^0 dh h^{-\alpha} \rho(r+h) \quad (42)$$

This at first abstract fractional derivative definition (42) allows a provisional physical interpretation:

We rewrite (42) as a sum

$$\rho^{(\alpha)} = \frac{1}{2} \frac{1}{\Gamma(1-\alpha)} \frac{\partial}{\partial r} \left(\int_\infty^0 dh h^{-\alpha} \rho(r-h) - \int_0^\infty dh h^{-\alpha} \rho(r+h) \right) \quad (43)$$

Within a classical picture [Ehrenfest (1927)], the fractional derivative is a weighted energy dependent sum of the projection of the density change along the classical trajectory expectation value of an incoming projectile, which runs from $\infty \leq$

$x \leq +\infty$ onto the radial vector. The weight function may be considered as the idealized hadronic analogue to a Bragg energy deposition curve, with a singularity at the position of closest approach to the origin [Bragg and Kleeman (1904), Bragg and Kleeman (1905), Wilson (1946)].

Note that due to our definition of a fractional derivative it follows a weak correspondence for α being even and odd respectively, if analytically continued from $0 < \alpha < 1$ to $\alpha > 0$:

$$\rho^{(\alpha)}(r) = \begin{cases} +\rho^{(n)}(r) & \alpha \rightarrow n, n \text{ even} \\ -\rho^{(n)}(r) & \alpha \rightarrow n, n \text{ odd} \end{cases} \quad (44)$$

which in a natural way yields the required sign change in (7), (25) and (27) for volume and surface part respectively.

Let us now apply (42) to the important case of a density of Woods-Saxon type

$$\rho_{WS}(r) = \rho_0 \left(1 + e^{\frac{r-R_0}{a_0}}\right)^{-1} \quad (45)$$

we obtain an analytic solution for the fractional derivative of ρ_{WS} according to (40):

$$\rho_{WS}^{(\alpha)}(r) = \frac{1}{\Gamma(1-\alpha)} \frac{\partial}{\partial r} \int_{\infty}^0 dh h^{-\alpha} \rho_{WS}(r+h), \quad 0 < \alpha < 1 \quad (46)$$

$$= -\rho_0 a_0^{1-\alpha} \frac{\partial}{\partial r} \text{Li}_{1-\alpha}(-e^{(R_0-r)/a_0}) \quad (47)$$

$$= -\rho_0 a_0^{-\alpha} \text{Li}_{-\alpha}(-e^{(R_0-r)/a_0}) \quad (48)$$

$$= \rho_0 a_0^{-\alpha} F_{-\alpha-1}((R_0-r)/a_0) \quad (49)$$

where $\text{Li}_{\gamma}(x)$ is the polylogarithm of fractional order γ , in our case with $-1 < \gamma < 0$ or equivalently from a physicist's point of view $F_{\beta}(x)$ is the Fermi-Dirac integral of fractional order β , in our case with $-2 < \beta < -1$, which occurred in physics at first for the special case $\beta = 1/2$ in the description of a degenerated electron gas in metals and later also within the framework of renormalization of quantum field theories [Pauli (1927), Sommerfeld (1928), Blakemore (1982), Sachdev (1993)].

As a side note, since the Fermi-Dirac integrals are given as

$$F_{\beta}(r) = \frac{1}{\Gamma(1-\beta)} \int_0^{\infty} dh h^{\beta} (1 + e^{h-r})^{-1}, \quad \beta > -1 \quad (50)$$

and the derivative follows from

$$F_{\beta(r)-1}(r) = \frac{\partial}{\partial r} F_{\beta}(r) \quad (51)$$

we may explicitly note:

$$F_{-\alpha-1}(r) = \frac{1}{\Gamma(1-\alpha)} \frac{\partial}{\partial r} \int_0^{\infty} dh h^{-\alpha} (1 + e^{h-r})^{-1}, \quad 0 \leq \alpha \leq 1 \quad (52)$$

Comparison with (40), (42), (46) leads to the conclusion: Everybody who uses fractional ($\alpha \notin \mathbb{Z}$) Fermi-Dirac or Bose-Einstein integrals is actually doing fractional calculus [NIST (2012), Millev (1996), Dingle (1957), Chaudhry and Qadir (2007)]!

Let us summarize our results obtained so far:

We have derived a closed formula for the fractional derivative of a Woods-Saxon type density in terms of fractional polylogarithms [Costin and Garoufalidis (2007), Tao (2022)], which allows for a smooth transition between the two extremal cases of volume and surface interpretation respectively.

Normalization of the density $\rho_{WS}^{(\alpha)}(r)$ may be achieved by integrating the density to obtain the correct number of protons/neutrons for a given nucleus. This integral may also be interpreted as a special case of a Mellin-transform [Mellin (1897)] of a Fermi-Dirac integral which has been considered by Dingle [Dingle (1957)].

$$\text{Vol}_{WS}(r, \alpha) = 4\pi \int_0^\infty r^2 dr \rho_{WS}^{(\alpha)}(r) \quad (53)$$

$$= 4\pi \int_0^\infty r^2 dr a_0^{-\alpha} \text{Li}_{-\alpha}(-e^{(R_0-r)/a_0}) \quad (54)$$

$$= 8\pi a_0^{3-\alpha} \text{Li}_{3-\alpha}(-e^{(R_0-r)/a_0}) \quad (55)$$

With the help of the asymptotic formula [Wood (1992)]

$$\lim_{w \rightarrow \infty} \text{Li}_p(\pm e^w) = -\frac{w^p}{\Gamma(1+p)} \quad p \neq -1, -2, \dots, -n \quad (56)$$

in the limit $a_0 \rightarrow \infty$ it follows for a homogeneous sphere with radius R_0 :

$$\text{Vol}_{WS}(r, \alpha) = \lim_{a_0 \rightarrow \infty} 8\pi a_0^{3-\alpha} \text{Li}_{3-\alpha}(-e^{(R_0-r)/a_0}) \quad (57)$$

$$= \frac{8\pi}{\Gamma(4-\alpha)} R_0^{3-\alpha} \quad (58)$$

which indeed yields the two limiting cases for volume and surface term normalization respectively:

$$\text{Vol}_{WS}(r, \alpha) = \begin{cases} \frac{4}{3}\pi R_0^3 & \alpha = 0 \\ 2\pi R_0^2 & \alpha = 1 \end{cases} \quad (59)$$

Let us finally connect the fractional derivative density $\rho_{WS}^{(\alpha)}(r)$ with the fractional optical potential absorption term V according to (37):

$$W^\alpha(r, \alpha) = W_\alpha a_0^\alpha \int_G \sqrt{g} dr' d\theta' d\phi' w(|r-r'|) \frac{\partial^\alpha}{\partial r'^\alpha} \rho(r') \quad (60)$$

$$= W_\alpha a_0^\alpha (w * \rho^{(\alpha)})(r) \quad (61)$$

$$= W_\alpha a_0^\alpha (w * w_L * \rho)(r) \quad 0 \leq \alpha \leq 1, \alpha \in \mathbb{R} \quad (62)$$

with only one parameter potential depth $W_\alpha(\alpha)$.

For the simplified case of an attractive contact interaction in spherical coordinates

$$w_\delta = w(r, r') = -\frac{1}{4\pi} \delta(|r-r'|) / \sqrt{g} \quad (63)$$

the corresponding fractional potential W_{WS}^α based on the Woods-Saxon type density $\rho_{WS}^{(\alpha)}(r)$ follows as:

$$W_{WS}^\alpha(r, \alpha) = W_\alpha a_0^\alpha \rho_{WS}^{(\alpha)}(r) \quad (64)$$

$$= W_\alpha \rho_0 \text{Li}_{-\alpha}(-e^{(R_0-r)/a_0}) \quad 0 \leq \alpha \leq 1 \quad (65)$$

where $\alpha = \alpha(E)$ is a function of energy.

In the top row of figure 2 we show a least square fit of the derived fractional Woods-Saxon potential from (65) with the absorption potential based on parameters from Becetti and Greensleves (10) for incident neutrons and protons respectively in the energy range $10 \leq E \leq 50$ [MeV] for Pb^{208} .

The graphs of the adjusted parameters $R_0, a_0, W_\alpha, \alpha$, of the new fractional potential are shown with solid lines in figures 7 and 8 for neutrons and protons

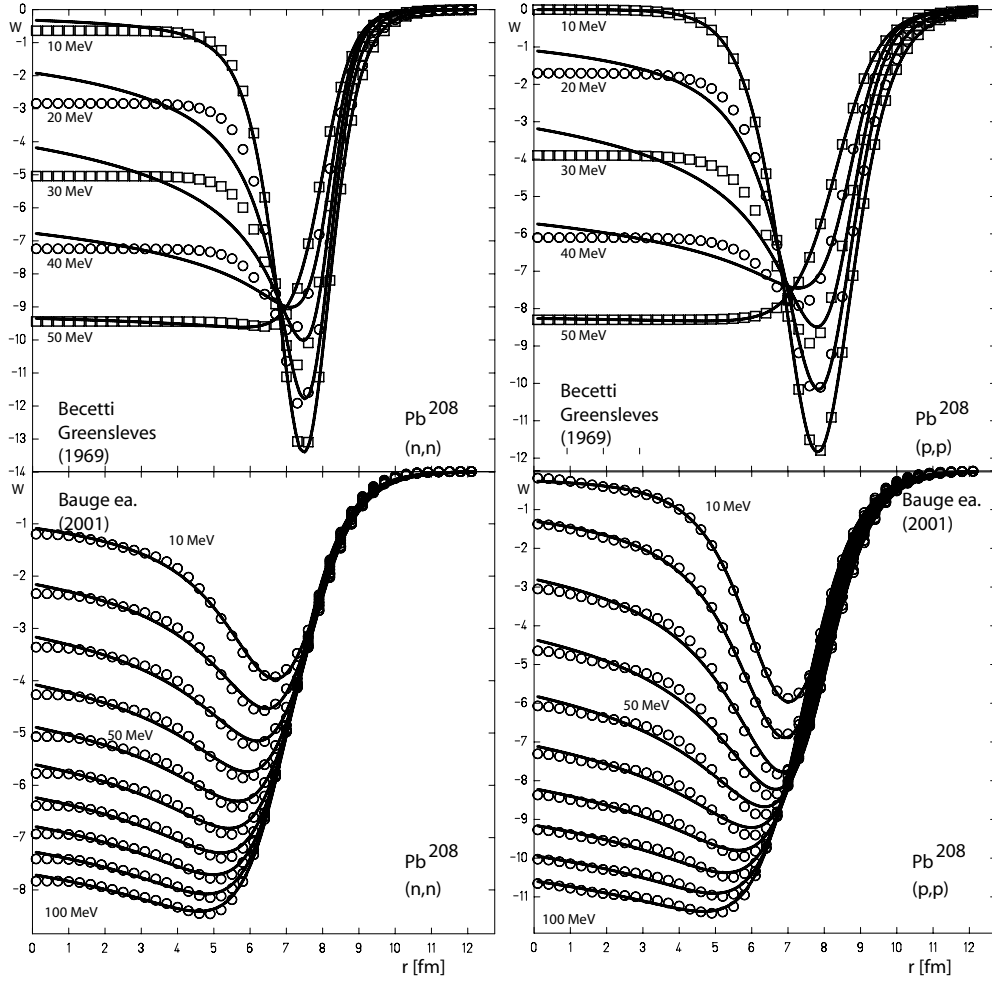


Figure 2. Top: Using parameters (10) from Becetti and Greenslevs the absorption potentials for incident neutrons (left side) and protons (right side) respectively are plotted in the energy range 10 – 50 MeV for Pb^{208} (circles and squares). Solid lines show the optimum fit in the range $0 < r < 2R_0$ for the proposed fractional derivative based potential (64).

Bottom: Using parameters derived from the microscopic model proposed by Bauge and co-workers [Bauge *et al* (1998), Bauge *et al* (2001)] the absorption potentials for incident neutrons and protons respectively are plotted in the energy range 10 – 100 MeV for Pb^{208} .

Circles indicate the original potential, solid lines the the optimum fit in the range $0 < r < 2R_0$ for the proposed fractional derivative based potential (64).

respectively. The energy dependence of α is nearly linear. Introducing a scaling factor e_0 [MeV] we obtain:

$$\alpha(E) \sim 1 - E/e_0 \quad 0 \leq E/e_0 \leq 1 \quad (66)$$

The gross features of both potential types are similar, indicating that the fractional approach leads to reasonable results. A significant difference shows up in the intermediate energy region inside the nucleus. Due to the simple form of the classical

absorption potential, which is only a superposition of the Woods-Saxon potential and its derivative, inside the nucleus there is only a constant contribution, while the fractional analogue shows a definite dominant decline with r in the inner region.

This behaviour is a direct consequence of the fractional approach which introduces a new quality named nonlocality when performing the convolution integral with the weakly singular kernel w_L and thus performing a infinite weighted sum of density values along the path.

The fractional approach anticipates the development of more sophisticated microscopic optical model potentials, where an effective nucleon-nucleon interaction is folded with the matter density distribution [Koning and Delaroche (2003)]. Both mechanisms introduce nonlocal aspects.

In the next section, we consider the consequences of a nonlocal approach.

6. Nonlocality - a comparison of the fractional approach to microscopic optical models

The optical model potential is both nonlocal and energy dependent. There are different levels of nonlocality:

On the highest level we may introduce nonlocal potentials and extend the Schrödinger equation (1) to an integro-differential equation as e.g. proposed by Perey and Buck [Perey and Buck (1962)]:

$$\left(-\frac{\hbar^2}{2m}\Delta - E\right)\Psi(\vec{r}, E) = - \int dr' U(\vec{r}, E)w(|r - r'|)\Psi(\vec{r}, E) \quad (67)$$

with a normalized non-singular kernel $w(x)$, e.g. a gaussian with a nonlocality spread $\sigma > 0$:

$$w(x) = \frac{1}{\sigma^3\pi\sqrt{\pi}}e^{-x^2/\sigma^2} \quad (68)$$

On a medium level we may consider folding the local density $\rho(\vec{r})$ with an appropriately chosen weight of Coulomb or effective nucleon-nucleon interaction w according to (14) in order to obtain a nonlocal potential. This level of nonlocality is realized for many microscopic or semi-microscopic optical models. [Jones (1963), Hodgson (1967), Rapaport *et al* (1986), Koning and Delaroche (2003), Mueller *et al* (2011), Koning *et al* (2014)].

Finally in the previous section we introduced an additional lower level of nonlocality by folding of the density $\rho(\vec{r})$ with a weakly singular kernel w_L to obtain an intermediate fractional derivative $\rho^{(\alpha)}(\vec{r})$.

As a consequence, the proposed fractional optical potential (60) is obtained by first folding the local density ρ_{WS} (45) of Woods-Saxon type with the nonlocal fractional derivative kernel w_L to obtain a nonlocal fractional density $\rho_{WS}^{(\alpha)}$ (46).

In a second step within for reasons of simplicity this nonlocal $\rho_{WS}^{(\alpha)}$ is folded with an attractive, but for now local contact potential $w_\delta(r, r')$ from (63) in spherical coordinates to obtain the fractional absorption potential W^α .

$$W^\alpha(r, \alpha) \sim (w_\delta * w_L * \rho_{WS})(r) \quad 0 \leq \alpha \leq 1, \alpha \in \mathbb{R} \quad (69)$$

Of course, nonlocal potential kernels may be used too.

In this section we will discuss the influence of this new nonlocality on the density level and compare it with the nonlocality on the potential level proposed within

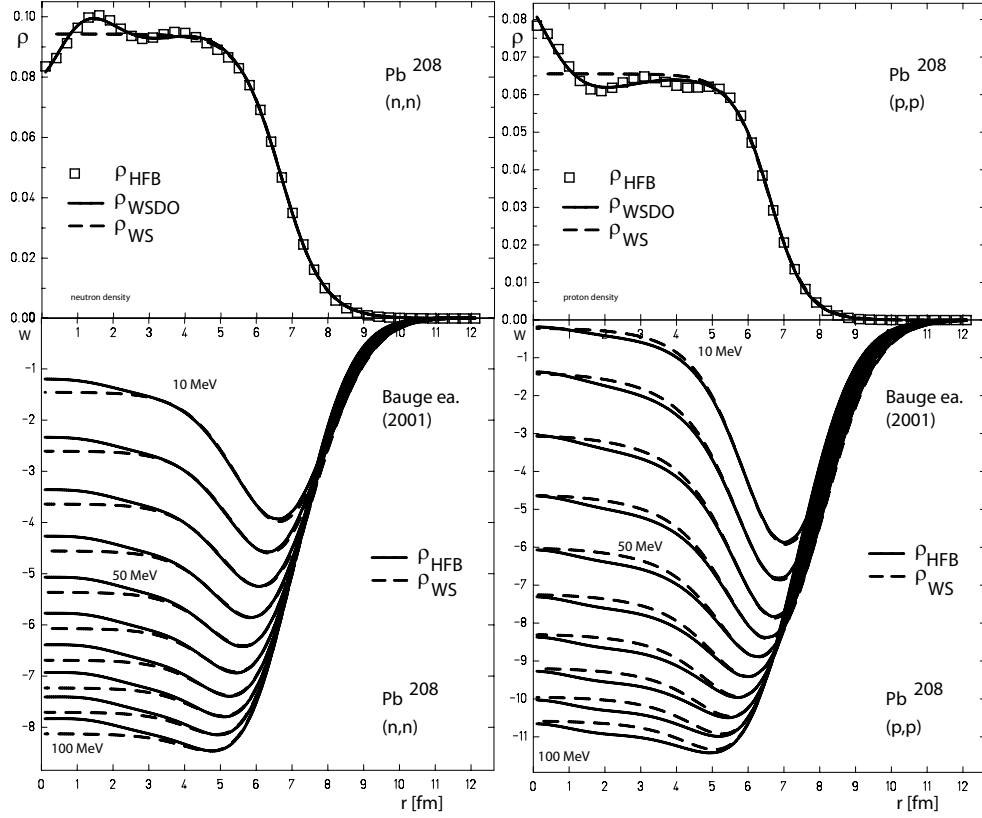


Figure 3. Top: Fit result for densities ρ_{HFB} of Pb^{208} published by Bauge and co-workers [Bauge (2001)] (marked by dots) with classical ($\alpha = 0$) Woods-Saxon density (46) (dashed line) and from (74) for classical ($\alpha = 0$) Woods-Saxon with damped oscillation admixture (solid line) for left/right neutrons/protons.

Bottom: The fitted densities served then as a basis to calculate the absorption potentials for Pb^{208} within the energy range of 10-100 MeV with software package MOM published by Bauge and co-workers [Bauge (2001)] the solid line shows the resulting potentials for the original density ρ_{HFB} the dashed curves show the deviation for the fitted classical Woods-Saxon density ($\alpha = 0$) and therefore the influence of oscillatory admixtures to the nucleon density on the absorption potential. Note the slope change in the inner region of the potential is almost missing for neutrons for ρ_{WS} but sets in for protons already for ρ_{WS} indicating the nonlocal character of the Coulomb force treatment.

a microscopic model. As an example in the following we compare with the well established microscopic model proposed by Bauge and co-workers [Bauge *et al* (1998), Bauge *et al* (2001)].

In general within the microscopic optical models there are two main optimizations included.

First, attempts are made to generate a more sophisticated density distribution for the nucleons and second, an appropriate collective effective nucleon potential is chosen, which is used for the folding procedure of the density to yield appropriate collective optical potential contributions. This folding procedure introduces the new concept of nonlocality into the optical model, provided that an appropriate nonlocal

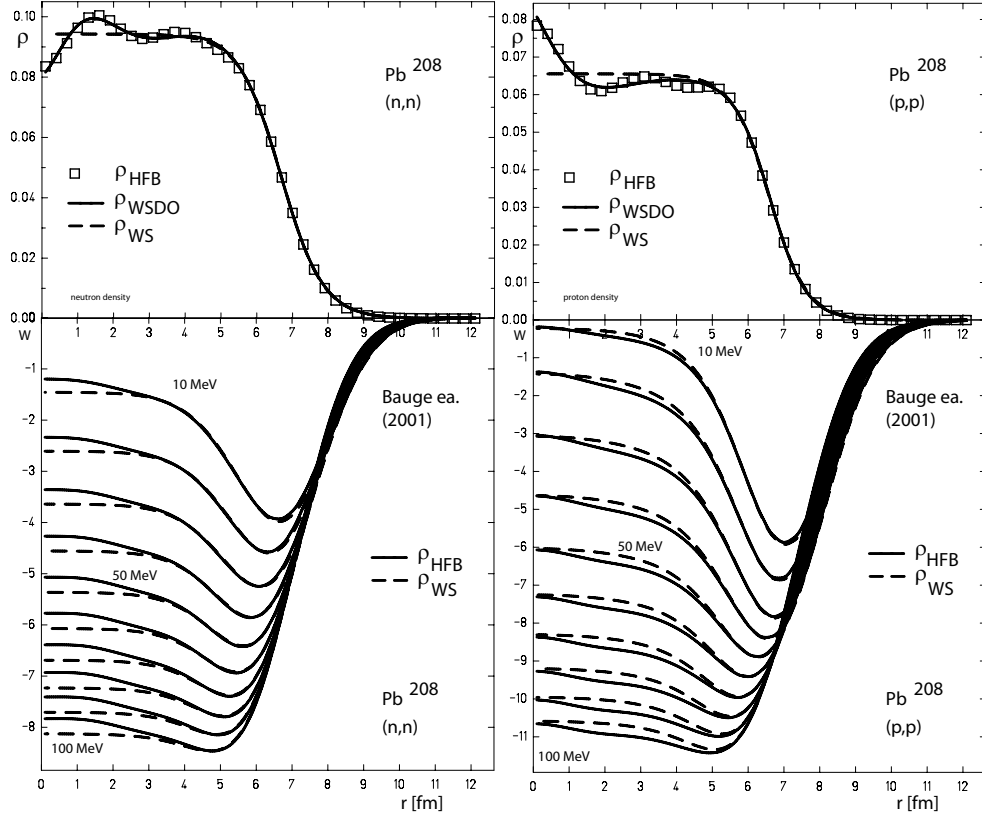


Figure 4. Top: Fit result for densities ρ_{HFB} of Pb^{208} published by Bauge and co-workers [Bauge (2001)] (marked by dots) with classical ($\alpha = 0$) Woods-Saxon density (46) (dashed line) and from (74) for classical ($\alpha = 0$) Woods-Saxon with damped oscillation admixture (solid line) for left/right neutrons/protons.

Bottom: The fitted densities served then as a basis to calculate the absorption potentials for Pb^{208} within the energy range of 10-100 MeV with software package MOM published by Bauge and co-workers [Bauge (2001)] the solid line shows the resulting potentials for the original density ρ_{HFB} the dashed curves show the deviation for the fitted classical Woods-Saxon density ($\alpha = 0$) and therefore the influence of oscillatory admixtures to the nucleon density on the absorption potential. Note the slope change in the inner region of the potential is almost missing for neutrons for ρ_{WS} but sets in for protons already for ρ_{WS} indicating the nonlocal character of the Coulomb force treatment.

kernel is used.

In order to generate the imaginary optical model potential contribution we use the code MOM [Bauge (2001)], which comes with a test file with precalculated neutron/proton densities for Pb^{208} which are folded with a modified effective nucleon interaction which yields corresponding optical model potentials.

In the bottom part of figure 2 we compare the absorption potentials from Bauge and co-workers [Bauge *et al* (2001)] (circles) with the fractional Woods-Saxon type potential (60) (solid lines). Both graphs agree much better over the whole energy range than in the case of Becetti's and Greensleves' potential see upper part if figure 2.

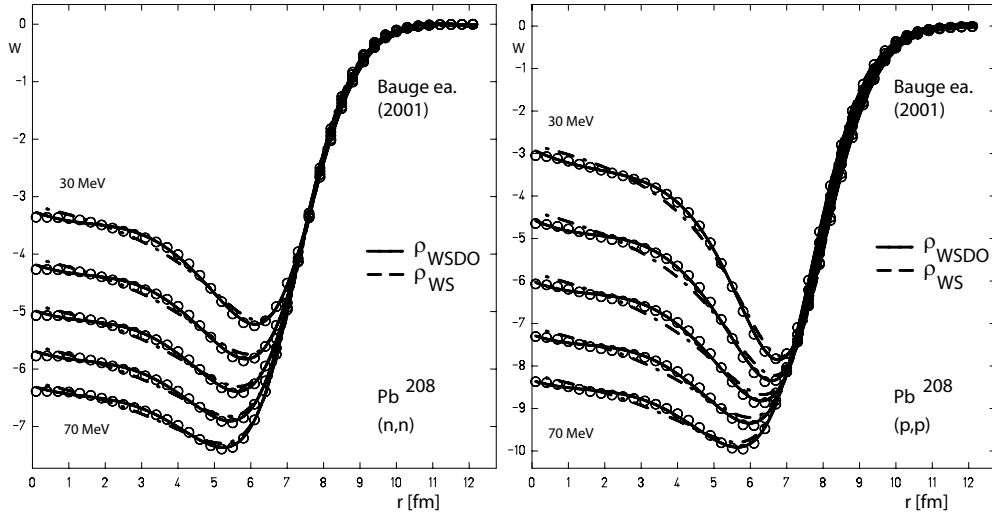


Figure 5. Fit result of the energy dependent absorption potential (circles) from Bauge and co-workers [Bauge *et al* (2001)] for Pb^{208} within the intermediate energy range 30-70 MeV with the fractional Woods-Saxon potential W_{WS}^α (65) (dashed lines), and with the fractional Woods-Saxon plus damped oscillation potential W_{WSDO}^α (76)(solid lines). The corresponding error is sketched in figure 6.

For both cases we observe a similar slope behaviour inside the target nucleus. Within the classical approach this behaviour sets in when the simple superposition of local volume and surface attribution is replaced by a more sophisticated non-local treatment of the potential in the microscopic models.

In the fractional approach nonlocality enters right from the beginning as a characteristic feature of the fractional derivative definition itself. On the other hand, in the classical derivation of the absorption potential according to microscopic models, nonlocality enters in MOM from Bauge and co-workers [Bauge *et al* (2001)] via the use of a nonlocal kernel of e.g. Gogny-type [Dechargè and Gogny (1980)] folding with a nucleon density, derived by HFB-calculations.

Formally written as

$$W(r, \alpha) \sim (w_{\text{Gogny}} * \rho_{\text{HFB}})(r) \quad (70)$$

where $\rho_{\text{HFB}}(r)$ is the input density .

Of course the question remains, what is the influence of the input density for the resulting absorption potential within the microscopic model considered.

In the upper row of figure 4 ρ_{HFB} from MOM from Bauge and co-workers [Bauge *et al* (2001)] is plotted with squares. We observe damped oscillatory admixtures to the simple Woods-Saxon density ρ_{WS} (dashed lines).

In the bottom row in figure 2 we compare the influence of oscillatory admixtures of the input density for the microscopic model calculations. The resulting absorption potential is plotted, which was calculated with MOM for the input densities of the standard Woods-Saxon type ρ_{WS} and $\rho_{\text{HFB}}(r)$.

The slope of the calculated absorption potential inside the nucleus is a direct property of the use of a microscopic model. Exactly this feature is missing using

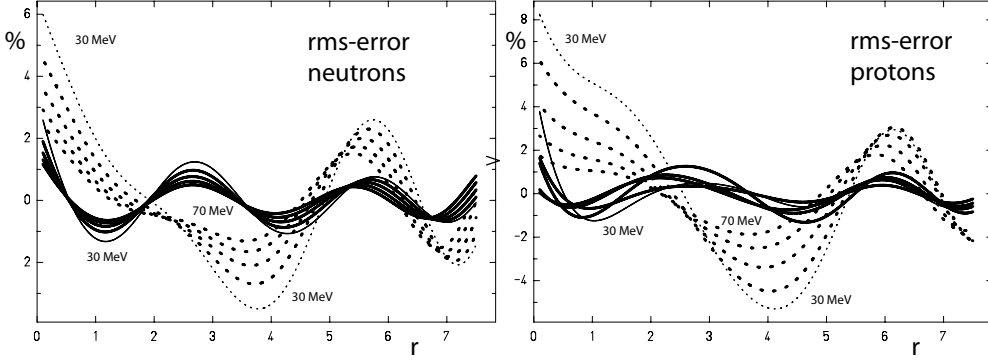


Figure 6. Root mean square error for the fits plotted in figure 5. Dashed lines show the error for the standard Woods-Saxon potential (65), solid lines show the error for for the extended Woods-Saxon plus damped oscillation potential (76). The overall agreement with the potential increases by a factor 2-3.

Beccetti's superposition ansatz, while the fractional potential W^α already shows this behaviour.

The presented results show, that the fractional approach implements right from the scratch while performing the step from ρ_{WS} to $\rho_{WS}^{(\alpha)}$ an nonlocal aspect to the absorption potential behaviour, which in the classical approach has to be modeled introducing additional nonlocal methods, e.g. folding with effective nucleon-nucleon interactions. The fractional Woods-Saxon potential, which is based on the nonlocal fractional Woods-Saxon type density, already anticipates nonlocal effects, which later in the development of the optical model occurred using more sophisticated microscopic models.

7. An extended Woods-Saxon potential with a damped oscillation term

Motivated by the functional behaviour of the more sophisticated density distribution from HFB-calculations, we now present a reasonable extension of the pure Woods-Saxon type densities, which will yield an even better agreement with the potentials presented by Bauge and co-workers [Bauge *et al* (2001)].

Extending the Woods-Saxon density (45) by a damped oscillatory part via

$$\rho_{WSDO} = \rho_{WS} + \rho_{DO} \quad (71)$$

where ρ_{DO} is given by

$$\rho_{DO}(r) = \rho_0 e^{-kr} \cos(mr + \phi) \quad \{k, m, \phi\} \in \mathbb{R}, \alpha, k > 0 \quad (72)$$

with a damping factor $k > 0$, oscillator frequency m and a phase ϕ .

Since the fractional derivative of the exponential is easily calculated with the help of (42):

$$\frac{\partial^\alpha}{\partial r^\alpha} e^{-kr+\phi} = k^\alpha e^{-kr+\phi} \quad \{k, \phi\} \in \mathbb{C}, \Re(\alpha, k) > 0 \quad (73)$$

we obtain for the fractional derivative of ρ_{DO} :

$$\rho_{DO}^{(\alpha)}(r) = \frac{1}{2} \rho_0 e^{-kx} \left(e^{i(mx+\phi)} (k - im)^\alpha + e^{-i(mx+\phi)} (k + im)^\alpha \right) \quad \{k, m, \phi\} \in \mathbb{R}, \alpha, k > 0 \quad (74)$$

$W_{index}^\alpha(r)$	α	R_0	a_0	W_α	W_\sim	k	m	ϕ	error
neutrons									
WS	0.253	7.35	0.670	10.08					7.2E-2
WSDO	0.285	7.21	0.744	10.44	0.22	0.076	0.96		2.7E-2
WSDO(P)	0.284	7.22	0.744	10.42	0.22	0.075	0.955	0.036	2.7E-2
protons									
WS	0.380	7.69	0.680	18.16					1.4E-1
WSDO	0.416	7.54	0.732	23.62	3.22	-0.18	0.41		2.7E-2
WSDO(P)	0.420	7.54	0.746	24.16	2.98	-0.13	0.42	-0.24	2.4E-2

Table 1. Example fit parameters for the absorption potential figure 5 for 40 MeV projectile energy. Listed are values for $W_{WS}^\alpha(r)$, the fractional standard Woods-Saxon potential $W_{WS}^\alpha(r)$ (65), $W_{WSDO}^\alpha(r)$ and $W_{WSDO(P)}^\alpha(r)$, the extended Woods-Saxon plus damped oscillation potential (76) without/with phase shift.

which is a real quantity, since for the complex conjugate $\overline{\rho_{DO}^{(\alpha)}}(r) = \rho_{DO}^{(\alpha)}(r)$ holds.

For the local contact kernel w_δ the fractional Woods-Saxon plus damped oscillation potential follows as:

$$\begin{aligned}
 W_{WSDO}^\alpha(r, \alpha) &= W_\alpha a_0^\alpha (w_\delta * \rho_{WSDO}^{(\alpha)})(r) & (75) \\
 &= a_0^\alpha \left(W_\alpha \text{Li}_{-\alpha}(-e^{(R_0-r)/a_0}) + \right. \\
 &\quad \left. + \frac{W_\sim}{2} e^{-kx} \left(e^{i(mx+\phi)} (k-im)^\alpha + e^{-i(mx+\phi)} (k+im)^\alpha \right) \right) \\
 &= a_0^\alpha \left(W_\alpha \text{F}_{-\alpha-1}((R_0-r)/a_0) + \right. \\
 &\quad \left. + \frac{W_\sim}{2} e^{-kx} \left(e^{i(mx+\phi)} (k-im)^\alpha + e^{-i(mx+\phi)} (k+im)^\alpha \right) \right) \\
 &\quad , \quad 0 \leq \alpha \leq 1, \alpha \in \mathbb{R} & (76)
 \end{aligned}$$

In figure 5 we compare the fractional standard Woods Saxon potential (64) and the extended Woods-Saxon potential (74) in the region 10-100 MeV projectile energy for the double magic Pb^{208} with the semi-microscopic absorption potential from [Bauge (2001)]. In figure 6 we plot the error for 30-70 MeV and in table 1 we list the fit parameters for the case 40 MeV in order to give an impression of the parameter change when applying the different model potentials.

Taking into account possible density fluctuations by extending the fractional Woods-Saxon potential by an additional term for fractional damped oscillations results in a potential model, which is flexible enough, to reduce the difference between the extended fractional and microscopic approach by an additional factor 2-3.

This allows a variation of the resulting fractional absorption potential similar to semi-microscopic models and opens a wide range of possible applications.

8. The fractional global parameter set

In the previous section we have applied the generated fractional model potential to a single nucleus using data for lead Pb^{208} as an example. Now we want to extend the

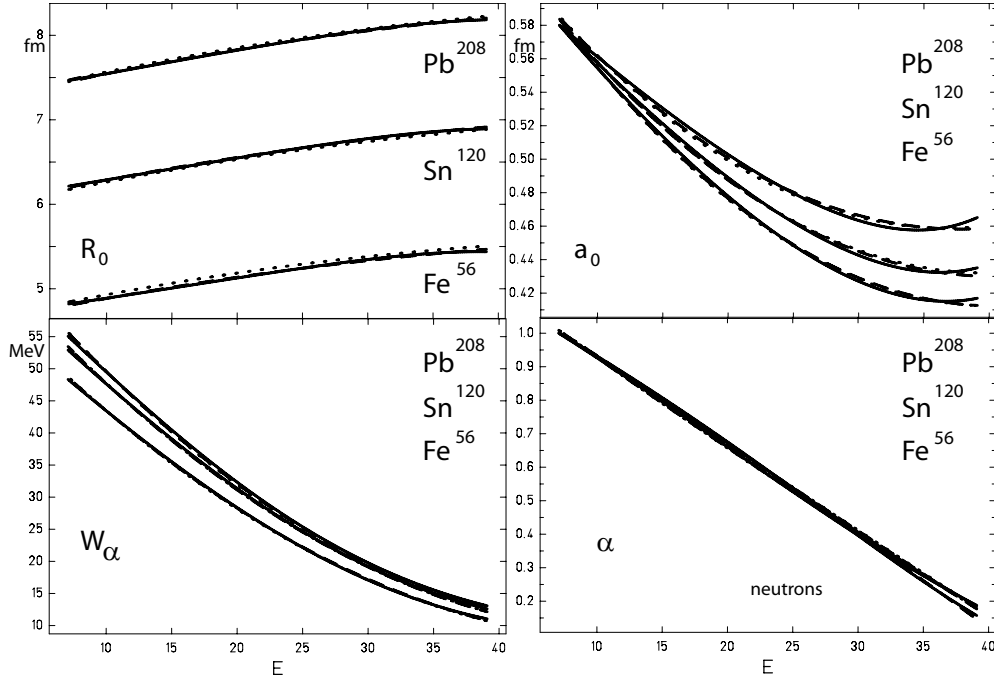


Figure 7. For R_0 , a_0 , W_α and α the global fit of the absorption potential according to (77) (solid line) with the potential based on the parameter set proposed by Becetti and Greensleves according to (10) (dashed line) is plotted for 3 different nuclei (Pb, Sn, Fe) in the energy range $10 \leq E \leq 40$ for incident neutron projectiles.

model parameter set to a wider range of nuclear targets.

Optimized parameter sets for the classical models have been reported for nucleon elastic scattering e.g. by [Becchetti and Greenlees (1969), Rapaport *et al* (1986), Walter and Guss (1986), Varner *et al* (1991), Koning and Delaroche (2003)] for a large variety of nuclei and energies. These were obtained by a fit with experimental cross sections and lead to corresponding optical potentials.

We will use a direct approach by fitting parameters for the previously derived fractional optical model potential directly with the classical optimal potential parameters given by Becetti and Greensleves according to (10).

We perform a two-step procedure: First for every valid projectile, energy and nuclear asymmetry combination we fit the classical absorption potential with the fractional Woods Saxon model. In the second step the resulting multi-dimensional point cluster is then fitted with an appropriately chosen fitting function.

As a fitting function ansatz which will minimize the error of the given fractional absorption potential (65) cluster we use an quadratic ansatz with parameters nucleon number A , asymmetry $I = (N - Z)/A$ and energy E :

$$f_\tau^\mu(A, I, E) = \sum_{i,j,k=0}^{i,j,k=2} b_{ijk} E^i I^j A^k, \quad (77)$$

$$\mu \in \{\alpha, a_0, R_0, W_\alpha\}$$

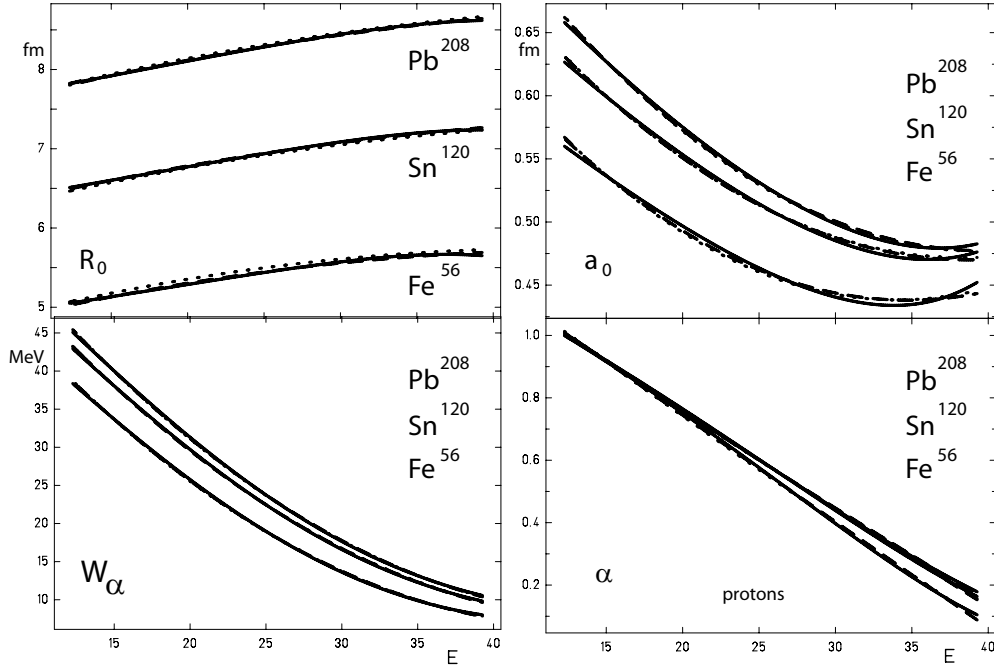


Figure 8. For R_0 , a_0 , W_α and α the global fit of the absorption potential according to (77) (solid line) with the potential based on the parameter set proposed by Becetti and Greensleves according to (10) (dashed line) is plotted for 3 different nuclei (Pb, Sn, Fe) in the energy range $10 \leq E \leq 40$ for incident proton projectiles.

$$\tau \in \{\text{neutrons, protons}\}$$

In tables 2 and 3 we have listed the adjusted b_{ijk} for α , R_0 , a_0 and W_α for neutrons and protons respectively. In figures 7 and 8 the corresponding graphs for the optimum parameter sets are plotted. The correspondence of our fractional model curves with the values proposed by Becetti (10) is remarkable.

For parameters α , R_0 , W_α of the fractional model we obtain an almost linear behaviour throughout the periodic table in the proposed energy region. It is noteworthy that especially the fractional parameter α shows a dominant linear dependence from energy almost independently of the target nucleus.

Of course this is only a coarse adjustment of the fractional parameters, because we compared results only on the potential level.

A next important step for future development will be a fine tuning of the fractional parameters based on the use of experimentally measured cross sections.

9. A-posteriori legitimation of the classical approach

Despite the fact, that the fractional derivative is the correct method to realize the intended smooth transition from surface to volume absorption potentials there remain open questions:

Why does the classical description of the same phenomenon in terms of a simple superposition of the first and zeroth derivative lead to comparable good results?

neutrons	μ			
	α	R_0	a_0	W_α
b_{000}	1.16002	3.23855	6.31512E-1	5.83134E1
b_{100}	-2.09028E-2	2.79605E-2	-7.64432E-3	-1.97058
b_{200}	-1.39729E-4	-2.26493E-4	1.09326E-4	1.87064E-2
b_{010}	-5.36764E-2	-4.36717E-1	2.12094E-1	4.68971E1
b_{110}	1.27116E-2	2.65314E-2	-1.84521E-2	2.50232E-1
b_{210}	1.88482E-4	-2.30697E-5	1.4966E-4	-2.36055E-2
b_{020}	-1.05737	5.21175	-2.16473	-2.15378E1
b_{120}	1.20967E-1	-6.0039E-1	2.65391E-1	3.2181
b_{220}	-3.00816E-3	1.2824E-2	-6.02127E-3	-6.33512E-2
b_{001}	9.60025E-4	2.61872E-2	4.3146E-4	2.39938E-2
b_{101}	-1.41237E-4	2.19149E-4	-7.05559E-5	-4.22499E-3
b_{201}	2.5512E-6	-3.698E-6	1.20596E-6	8.4832E-5
b_{011}	-2.30815E-3	6.80988E-3	-2.49754E-4	9.36127E-2
b_{111}	3.34947E-4	-9.15282E-4	1.39433E-4	-5.23342E-3
b_{211}	-7.41202E-6	1.77282E-5	-3.16304E-6	5.68913E-5
b_{021}	1.36172E-2	-5.81241E-2	1.76318E-2	-1.02795E-1
b_{121}	-1.76209E-3	7.27927E-3	-2.49776E-3	-1.11364E-2
b_{221}	4.02172E-5	-1.61211E-4	5.92301E-5	3.87674E-4
b_{002}	-1.70111E-6	-3.67824E-5	-7.23149E-7	-3.58834E-5
b_{102}	2.47862E-7	-4.0281E-7	1.26007E-7	6.93429E-6
b_{202}	-4.31213E-9	6.61254E-9	-2.1266E-9	-1.36821E-7
b_{012}	4.73126E-6	-1.62584E-5	-9.71364E-7	-3.56636E-4
b_{112}	-7.41566E-7	2.40676E-6	-3.18572E-7	2.02272E-5
b_{212}	1.60083E-8	-4.79778E-8	8.58725E-9	-2.79077E-7
b_{022}	-2.99806E-5	1.31688E-4	-2.86779E-5	9.99785E-4
b_{122}	4.14497E-6	-1.7493E-5	5.08152E-6	-2.76855E-5
b_{222}	-9.54636E-8	3.92787E-7	-1.27997E-7	2.01557E-8

Table 2. Fit parameters b_{ijk} according to (77) for neutrons

Is this a special case for functions of Woods-Saxon type only?

In the following we will give an answer presenting a different interpretation of a fractional derivative, which is based on an infinite series expansion of the fractional derivative in terms of integer derivatives.

At first glance it is tempting to assume the fractional calculus approach to derive a reasonable optical potential as a fractional derivative of the nuclear density function would be a simple series expansion of the same derivative in terms of integer derivatives

$$\rho^{(\alpha)}(x) \stackrel{?}{=} \sum_{i=0}^{\infty} \tilde{c}_i(\alpha) \rho^{(i)}(x) \quad (78)$$

with spatially independent coefficients $\tilde{c}_i(\alpha)$. The classical approach was then interpreted as a truncation of this series to two terms only, namely $i \leq 1$ for the zeroth and first derivative of the density function.

In fractional calculus things are not that simple. One of the premises for any reasonable definition of a fractional derivative is that the fractional extension of the classical Leibniz product rule is to be fulfilled, which is given by:

$$(\psi \chi)^{(\alpha)}(x) = \sum_{j=0}^{\infty} \binom{\alpha}{j} \psi^{(\alpha-j)}(x) \chi^{(j)}(x) \quad (79)$$

protons	μ			
	α	R_0	a_0	W_α
b_{000}	1.45738	2.97928	6.91304E-1	6.22561E1
b_{100}	-3.57272E-2	5.61629E-2	-1.73707E-2	-2.54804
b_{200}	-1.52847E-5	-6.78655E-4	2.71946E-4	2.87836E-2
b_{010}	-1.73192	2.17068	3.82327E-2	1.89994E1
b_{110}	1.55702E-1	-2.18343E-1	6.80405E-2	3.28564
b_{210}	-2.0218E-3	4.64791E-3	-1.47557E-3	-8.31024E-2
b_{020}	2.79229	-3.24036	9.68804E-1	2.80201E1
b_{120}	-2.6603E-1	3.36065E-1	-1.01722E-1	-3.36481
b_{220}	4.72882E-3	-7.92969E-3	2.43325E-3	9.59847E-2
b_{001}	2.60798E-3	2.47759E-2	1.33373E-3	5.46996E-2
b_{101}	-2.64892E-4	4.22512E-4	-1.35713E-4	-5.91297E-3
b_{201}	4.94074E-6	-7.91767E-6	2.52546E-6	1.15096E-4
b_{011}	-6.62564E-3	1.46379E-2	-3.2664E-3	3.00421E-2
b_{111}	7.43875E-4	-1.52236E-3	3.51202E-4	-6.14844E-4
b_{211}	-1.81707E-5	3.72658E-5	-9.11869E-6	-7.04581E-5
b_{021}	6.71699E-3	-2.75892E-2	5.68185E-3	-1.28594E-1
b_{121}	-8.09413E-4	2.78814E-3	-5.82523E-4	1.03988E-2
b_{221}	2.20862E-5	-6.63321E-5	1.45556E-5	-1.46995E-4
b_{002}	-6.07232E-6	-2.85172E-5	-4.5608E-6	-1.24689E-4
b_{102}	6.01584E-7	-1.25619E-6	4.47185E-7	1.29714E-5
b_{202}	-1.14806E-8	2.48641E-8	-8.89248E-9	-2.55434E-7
b_{012}	3.11991E-5	-9.71514E-5	3.37022E-5	3.20899E-4
b_{112}	-3.159E-6	9.46288E-6	-3.2767E-6	-3.44315E-5
b_{212}	7.16834E-8	-2.12167E-7	7.35789E-8	8.89428E-7
b_{022}	-6.24725E-5	2.38078E-4	-8.37765E-5	-7.11391E-4
b_{122}	6.24831E-6	-2.2947E-5	8.04581E-6	7.14510E-5
b_{222}	-1.43356E-7	5.07704E-7	-1.78026E-7	-1.69351E-6

Table 3. Fit parameters b_{ijk} according to (77) for protons

Rewriting the analytic function $\rho(x)$ as a general product:

$$\rho(x) = \lim_{\beta \rightarrow 0} x^\beta \rho(x) = x^0 \rho(x) \quad \beta, x \geq 0 \quad (80)$$

or equivalently setting $\psi(x) = x^0 = 1$ and consequently interpreting the term $\partial_x^{\alpha-j} \psi(x)$ as the fractional integral of a constant function proves its x dependence even for the case of integer α , $\alpha = n \in \mathbb{N}$. So, although that the fractional extension of the Leibniz product rule is the correct starting point for a series expansion of the fractional derivative in term of integer derivatives, we obtain space dependent coefficients $c_i(\alpha, x)$.

$$\rho^{(\alpha)}(x) \stackrel{!}{=} \sum_{i=0}^{\infty} c(\alpha, x) \rho^{(i)}(x) \quad (81)$$

Nevertheless, we propose two approaches to eliminate the spatial dependence of the coefficients in (81). The first approach is based on the Gaussian least squares method determining the coefficients $\tilde{c}_i(\alpha)$ within a given interval $[a, b]$ as solutions of

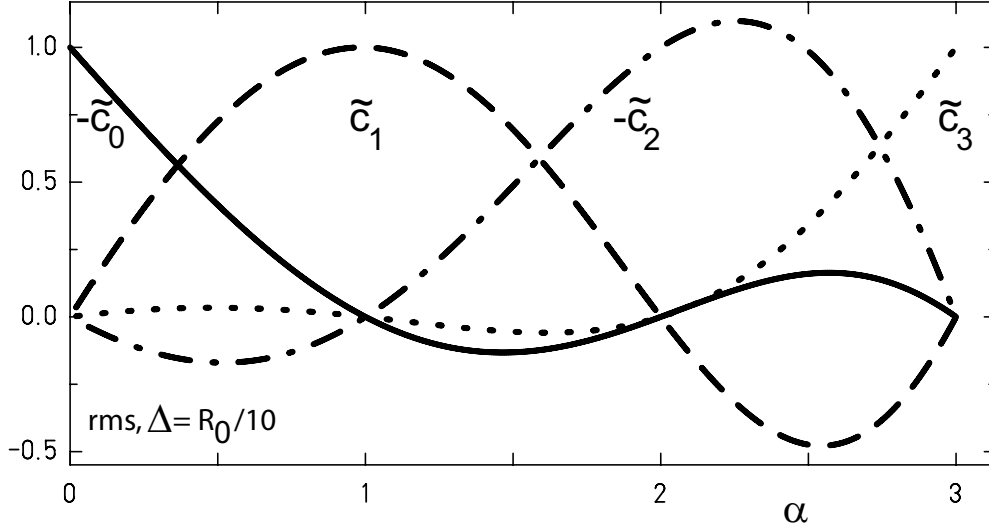


Figure 9. For ^{208}Pb coefficients \tilde{c}_j as a function of α from optimum fit of the fractional Woods-Saxon potential $\rho_{WS}^{(\alpha)}(r)$ from (46) in the vicinity $\Delta = R_0/10$ of R_0 . Signs are adjusted such that $\tilde{c}_j(\alpha) = 1$ for $\alpha = j$. The relevant region $0 < \alpha < 1$ may be directly compared with the classical linear ansatz e.g. (8) or (10)

the overdetermined system of equations ($N \gg M \in \mathbb{N}$):

$$\delta \sum_{i=0}^{(b-a)/N} \left(\rho^{(\alpha)}(x_i) - \sum_{i=0}^M \tilde{c}_i(\alpha) \rho^{(i)}(x) |_{x_i} \right)^2 = 0 \quad (82)$$

Especially for the Woods-Saxon type functions we will focus on the vicinity of $x = x_s = R_0$, since only at this point we expect a significant contribution of higher order integer derivatives, while for $x \rightarrow 0$ and $x \rightarrow \infty$ the higher order derivatives ($i > 0$) are negligible. We therefore postulate, that a valid comparison of contributions of higher order derivatives makes sense only in the vicinity of R_0 .

Setting $M = 4$, $a = R_0 - \Delta$, $b = R_0 + \Delta$ with $\Delta = 0.1R_0$ and $N = 100$ we obtain the set $\{\tilde{c}_0(\alpha), \tilde{c}_1(\alpha), \tilde{c}_2(\alpha), \tilde{c}_3(\alpha)\}$. In figure 9 the parameter values for Pb^{208} are plotted.

Before we discuss this result, let us take a look at the second approach:

We will derive an alternative definition of a fractional derivative in terms of a sum of integer derivatives localized at a given position $x = x_s$, which allows a comparison with the above presented first approach.

$$\frac{\partial^\alpha}{\partial x^\alpha} f(x) |_{x=x_s} = \sum_{j=0}^{\infty} c_j(x) \frac{\partial^j}{\partial x^j} f(x) |_{x=x_s} \quad 0 \leq \alpha \leq 1 \quad (83)$$

$$= c_0(x) f(x) + c_1(x) \frac{\partial}{\partial x} f(x) + I(x, \alpha) |_{x=x_s} \quad (84)$$

with a residual $I(x_s, \alpha)$.

We will then demonstrate, that the hitherto used classical approach covers the first two terms of this series expansion only, which at first seems quite a poor

approximation. After that we will then derive an error estimate and will deduce, that the contribution of higher order terms in the series expansion are surprisingly small for Woods-Saxon type functions for α in the range $0 \leq \alpha \leq 1$.

For Woods-Saxon type densities there are two conditions fulfilled:

First there exists a mirror point x_s with the property:

$$2\rho(x_s) = \rho(x_s + h) + \rho(x_s - h) \quad (85)$$

In the special case of the Woods-Saxon type density $x_s = R_0$.

Second, we have an asymptotic development of the form $\lim_{r \rightarrow \infty} \rho_{WS} = 0$ and introducing the residual $R(\alpha, x_s)$

$$R(\alpha, x_s) = \partial_{x_s} \int_{x_s}^{\infty} dh \frac{1}{h^\alpha} \rho(x+h) < \epsilon \quad (86)$$

we have $R(\alpha, x_s) < \epsilon$ such that

$$\partial_x \int_0^{\infty} dh \frac{1}{h^\alpha} \rho(x+h) = \partial_x \int_0^{x_s} dh \frac{1}{h^\alpha} \rho(x+h) + R(\alpha, x_s) \quad (87)$$

$$\approx \partial_x \int_0^{x_s} dh \frac{1}{h^\alpha} \rho(x+h) \quad (88)$$

That indeed shows that for the Woods-Saxon density ρ_{WS} the residual is nothing else but the upper incomplete polylogarithm and we can give an upper estimate for ϵ using properties of the exponential integral $E_\alpha(x)$

$$R(\alpha, x_s) = \partial_{x_s} \frac{1}{\Gamma(1-\alpha)} \int_{x_s}^{\infty} dh \frac{1}{h^\alpha} \frac{1}{1 + e^{(R_0-x)/a_0}} \quad (89)$$

$$< \partial_{x_s} \frac{1}{\Gamma(1-\alpha)} \int_{x_s}^{\infty} dh \frac{1}{h^\alpha} e^{-(R_0-x)/a_0} \quad (90)$$

$$= e^{\frac{R_0-x_s}{a_0}} \frac{x_s^{-\alpha}}{\Gamma(1-\alpha)} \left(1 + \frac{x_s}{a_0} e^{x_s/a_0} E_\alpha(x_s/a_0)\right) \quad (91)$$

which at $x_s = R_0$ results in

$$R(\alpha, x_s) < R(0, x_s) < \epsilon = 2e^{-\frac{R_0}{a_0}} \quad (92)$$

In practice this yields a value $\epsilon \approx 4.0 \times 10^{-3}$ for Ca^{40} and $\epsilon \approx 5.0 \times 10^{-5}$ for Pb^{208} respectively, a contribution, that is in fact negligible compared to the exact value which is of order 1. Now with (85) we obtain for (88)

$$\begin{aligned} \partial_x \frac{1}{\Gamma(1-\alpha)} \int_0^{\infty} dh \frac{1}{h^\alpha} \rho(x+h) \Big|_{x=x_s} &\approx \\ \partial_{x_s} \frac{1}{\Gamma(1-\alpha)} \int_0^{x_s} dh \frac{1}{h^\alpha} (2\rho(x_s) - \rho(x_s-h)) &\approx \end{aligned} \quad (93)$$

$$2\rho(x_s) \partial_{x_s} \frac{1}{\Gamma(1-\alpha)} \int_0^{x_s} dh \frac{1}{h^\alpha} - \partial_{x_s} \frac{1}{\Gamma(1-\alpha)} \int_0^{x_s} dh \frac{1}{h^\alpha} \rho(x_s-h) \approx \quad (94)$$

$$2\rho(x_s) \frac{x_s^{-\alpha}}{\Gamma(1-\alpha)} - \partial_{x_s} \frac{1}{\Gamma(1-\alpha)} \int_0^{x_s} dh \frac{1}{h^\alpha} \rho(x_s-h) \quad (95)$$

The last term in (95) is nothing else but the Riemann definition of a fractional derivative at x_s [Riemann (1847)]:

$${}_R \partial_x^\alpha \rho(x) = \partial_x \frac{1}{\Gamma(1-\alpha)} \int_0^x dh \frac{1}{h^\alpha} \rho(x-h) \quad (96)$$

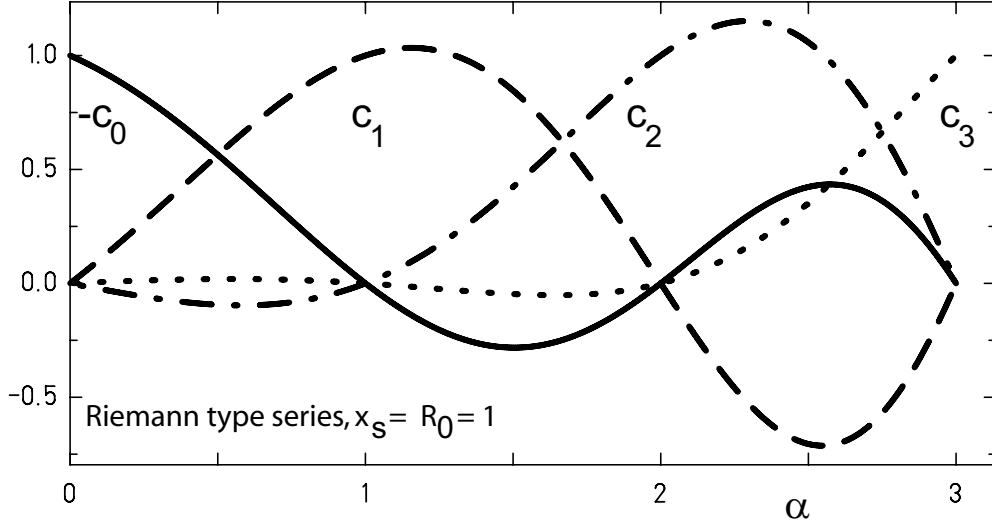


Figure 10. For ^{208}Pb coefficients c_i as a function of α from the series expansion of the fractional Woods-Saxon potential $\rho_{WS}^{(\alpha)}(r)$ from (46) in terms of integer derivatives of order j at $\tilde{x}_s = 1$, see (100). Signs are adjusted such that $c_j(\alpha) = 1$ for $\alpha = j$. The relevant region $0 < \alpha < 1$ may be directly compared with the classical linear ansatz e.g. (8) or (10).

With the property that the integral converges for $\rho(x) = x^\beta$, even for $\beta = 0$:

$${}_R\partial_x^\alpha x^\beta = \frac{\Gamma(1+\alpha)}{\Gamma(1+\alpha-\beta)} x^{\beta-\alpha}, \quad \beta \geq 0 \quad (97)$$

The Leibniz product rule then follows as [Herrmann (2018)]

$${}_R\partial_x^\alpha \rho(x)|_{x=x_s} = x^{-\alpha} \sum_{j=0}^{\infty} \binom{\alpha}{j} \frac{1}{\Gamma(1-\alpha+j)} x^j \partial_x^j \rho(x) \Big|_{x=x_s} \quad (98)$$

Thus we finally obtain

$$\begin{aligned} & \partial_x \frac{1}{\Gamma(1-\alpha)} \int_0^\infty dh \frac{1}{h^\alpha} \rho(x+h)|_{x_s} \\ & \approx 2\rho^{(0)}(x_s) \frac{x_s^{-\alpha}}{\Gamma(1-\alpha)} - x_s^{-\alpha} \sum_{j=0}^{\infty} \binom{\alpha}{j} \frac{1}{\Gamma(1-\alpha+j)} x_s^j \rho^{(j)}(x_s) \\ & = \rho^{(0)}(x_s) \frac{x_s^{-\alpha}}{\Gamma(1-\alpha)} - x_s^{-\alpha} \sum_{j=1}^{\infty} \binom{\alpha}{j} \frac{1}{\Gamma(1-\alpha+j)} x_s^j \rho^{(j)}(x_s) \end{aligned} \quad (99)$$

which is the series expansion of our Liouville type fractional derivative in terms of ordinary integer derivatives $\rho^{(n)}(x_s)$ of order n at $x = x_s = R_0$, with accuracy given by $R(\alpha, x_s) < \epsilon$. In order to compare the different coefficients we perform a scaling transformation of the form

$$\tilde{x}_s = x_s/R_0 \quad (100)$$

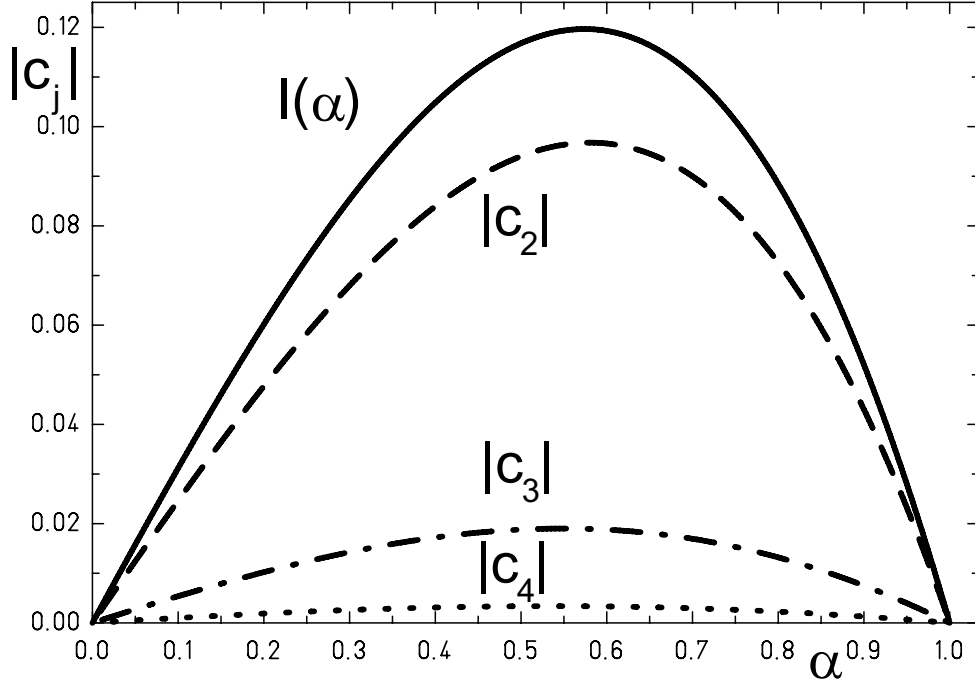


Figure 11. Dashed lines show coefficients c_j with $j \geq 2$ as a function of α from (104) and the solid line represents the residue $I(x_s, \alpha)$ from (108).

and set $\tilde{x}_s = 1$. An approximate analytic expression for the coefficients c_j follows as

$$\begin{aligned} \rho^{(\alpha)}(\tilde{x})|_{\tilde{x}=1} &\approx \frac{1}{\Gamma(1-\alpha)}\rho^{(0)}(\tilde{x})|_{\tilde{x}=1} - \frac{\alpha}{\Gamma(2-\alpha)}\rho^{(1)}(\tilde{x})|_{\tilde{x}=1} \\ &\quad - \sum_{j=2}^{\infty} \binom{\alpha}{j} \frac{1}{\Gamma(1-\alpha+j)}\rho^{(j)}(\tilde{x})|_{\tilde{x}=1} \quad (101) \\ &= \sum_{j=0}^{\infty} c_j \rho^{(j)}(\tilde{x})|_{\tilde{x}=1} \quad (102) \end{aligned}$$

We get an analytic expression for the coefficients

$$c_j = \begin{cases} +1/\Gamma(1-\alpha) & j=0 \\ -\binom{\alpha}{j}/\Gamma(1-\alpha+j) & j>0 \end{cases} \quad (103)$$

For the lowest coefficients we explicitly obtain:

$$c_j = \begin{cases} +1/\Gamma(1-\alpha) & j=0 \\ -\alpha/\Gamma(2-\alpha) & j=1 \\ +\frac{1}{2}\alpha(1-\alpha)/\Gamma(3-\alpha) & j=2 \\ -\frac{1}{6}\alpha(1-\alpha)(2-\alpha)/\Gamma(4-\alpha) & j=3 \end{cases} \quad (104)$$

In figure 10 we have plotted these coefficients.

Since the Riemann fractional derivative (96) applied to the exponential is given by:

$${}_R\partial_r^\alpha e^{-kr} = r^\alpha E_{1,1-\alpha}(-kr) \quad (105)$$

$$= (-k)^\alpha e^{-kr} \left(1 - \frac{\alpha \Gamma(-\alpha, -kr)}{\Gamma(1-\alpha)}\right) \quad (106)$$

$$= (-k)^\alpha e^{-kr} Q(-\alpha, 0, -kr) \quad k, r \geq 0 \quad (107)$$

where $E_{\alpha,\beta}(z)$, $\Gamma(a, z)$ and $Q(a, z_0, z_1)$ are the generalized Mittag-Leffler-[Mittag-Leffler (1903), Wiman (1905)], the incomplete Γ - and the generalized regularized incomplete Γ -function [Wolfram (2022)], we may easily obtain an analytical estimate for the influence $I(\alpha)$ of the higher order derivative contributions. We calculate the sum of the absolute values of the coefficients c_j :

$$I(x_s, \alpha) = \sum_{j=2}^{\infty} \left| \binom{\alpha}{j} \frac{1}{\Gamma(1-\alpha+j)} \right| \quad (108)$$

$$= \sum_{j=0}^{\infty} (-1)^j \binom{\alpha}{j} \frac{1}{\Gamma(1-\alpha+j)} - c_0 - c_1 \quad (109)$$

$$= (-1)^\alpha Q(-\alpha, 0, -1) + \frac{1}{\Gamma(1-\alpha)} - \frac{\alpha}{\Gamma(2-\alpha)} \quad (110)$$

Within the relevant region $0 \leq \alpha \leq 1$ this function is extremal at $I(\alpha = 0.58) \approx 0.12$, while $|c_0| + |c_1| \approx 1$. Therefore we obtain the result, that the contribution of higher order integer derivatives beyond $j = 1$ is about 10% of the $j = 0, 1$ part. What we have not taken into account are higher order function derivatives $f^{(j>1)}$ and their influence on the total fractional derivative $f^{(\alpha)}$. In addition, our derivation is restricted to the close vicinity of R_0 which once again shows the limitations of a local approach.

Therefore we may deduce, that in the case of classical Woods-Saxon type functions, which fulfil the requirements (85) and (86) the classical approach to generate the absorption part of the optical potential as a superposition of the original function and its first derivative may be considered as the lowest order local approximation to an a priori nonlocal problem, the smooth transition from surface to volume absorption.

The fractional derivative approach automatically implies a nonlocal view to the same problem and offers a consistent solution without previously made simplifications, which were necessary for the classical approach.

It is a special property of the Woods-Saxon type functions, that the practical differences of both approaches turn out to be small in the cases considered so far.

10. Conclusion

The optical model plays a fundamental role in interpreting scattering data in nuclear and particle physics. In order to achieve conformity with experimental findings, the absorption process may be understood assuming a smooth transition from surface to volume absorption with increasing energy of the incident particle.

In this paper we proposed a new and as we think only appropriate treatment of this problem.

Based on the observation, that a surface may be considered as a more or less drastic change of a given density and the fact, that such a change may be described using methods of vector calculus we introduced a fractional gradient definition based

on methods developed in fractional calculus, which allows to determine the required smooth transition from volume to surface potentials.

We derived closed form solutions for the practically important cases of Woods-Saxon and Woods-Saxon-plus-damped-oscillation functions in terms of higher order transcendental functions namely polylogarithms.

We applied these new fractional potentials to macroscopic and semi-microscopic nonlocal models and found, that nonlocal effects, which are a natural property of the fractional approach, are particularly well reproduced.

We finally showed, that the hitherto accepted classical solution, which is a simple superposition of a Woods-Saxon function and its derivative may be considered as the lowest order local approximation to the full nonlocal problem.

We have demonstrated that a complete solution of this problem can be formulated adequately within the framework of fractional calculus.

This paper is also a plea for optimism and a lesson how progress in physics evolves as well [Dirac (1984), Hossenfelder (2018)]:

More than 60 years ago, a first solution for optical absorption potentials was proposed, which since then has been used to categorize and interpret experimental data. Since then, this problem was considered as solved and consequently there was no demand for a more sophisticated solution nor a different vista.

Now a new point of view based on fractional calculus is leading to new insights and surprising interrelations on this classical field of research.

It should be emphasized, that the presented fractional approach is not just one more method to describe a smooth transition from surface to volume dependence, it is the only one up to now which fulfils the claim for an appropriate treatment of the problem and of course, may be and will be applied to other research fields as well.

The presented results encourage further research in this field. A necessary next step will be to use the presented fractional potentials to serve as a basis for the interpretation of experimental cross-sections and also an extension of the formalism to projectile/target combinations beyond nucleon/nucleus combinations.

11. Acknowledgments

This article is the elaborated version of a talk prepared for the workshop *Fractional Differential Equations* planned at the Isaac Newton Institute for Mathematical Sciences (INI), Cambridge UK from 4 January 2021 to 30 April 2021, but cancelled due to corona pandemic.

We thank A. Friedrich for support and useful discussions. Numerical calculations were partly performed on the π -dron-cluster at the HPC testing facilities at gigahedron, Germany.

12. Bibliography

- [Abbot *et al* (2017)] Abbot, LIGO Scientific Collaboration and Virgo Collaboration (2017). *GW170817: Observation of gravitational waves from a binary neutron star inspiral* Phys. Rev. Lett. **119**, 161101,
- [Aleksandrov *et al* (2022)] Aleksandrov, I. A. Di Piazza, A. and Plunien, G. and Shabaev, V. M. (1977). *Stimulated vacuum emission and photon absorption in strong electromagnetic fields* Phys. Rev. D. **105**, 116005, 13pp.
- [Altarelli and Parisi (1977)] Altarelli, G. and Parisi, G. (1977). *Asymptotic freedom in parton language* Nucl. Phys. **126**, 298–318,
- [Bacon (1267)] Bacon, R. (1267) *Opus majus* Translated by Robert Belle Burke, Cambridge Library Collection - Physical Sciences, Cambridge University Press (2010)
- [Bauge *et al* (1998)] Bauge, E., Delaroche, J. P. and Girod, M. (1998). *Semimicroscopic nucleon-nucleus spherical optical model for nuclei with $A > 40$ at energies up to 200 MeV* Phys. Rev. C **58**, 1118–1145,
- [Bauge *et al* (2001)] Bauge, E., Delaroche, J. P. and Girod, M. (2001). *Lane-consistent, semi microscopic nucleon-nucleus optical model* Phys. Rev. C **63**, 024607,
- [Bauge (2001)] Bauge, E., Delaroche, J. P. and Girod, M. (2001). *The MOM semi microscopic optical model potential program* Phys. Rev. C **63**, 024607,
- [Becchetti and Greenlees (1969)] Becchetti, F. D. and Greenlees, G. W. (1969). *Nucleon-nucleus optical-model parameters, $A > 40$, $E < 50$ MeV* Phys. Rev. **182**, 1190–1209,
- [Becquerel (1896)] Becquerel, H. (1896). *Sur les propriétés différentes des radiations invisibles émises par les sels d'uranium* Compt. Rendus. T. **122**, 689–694,
- [Berger *et al* (1991)] Berger, J. F., Girod, M. and Gogny, D. M. (1991). *Time-dependent quantum collective dynamics applied to nuclear fission* Comp. Phys. Comm. **63**, 365–374,
- [Bethe (1940)] Bethe, H. A. (1940). *A continuum theory of the compound nucleus* Phys. Rev. **57**, 1125–1144,
- [Blakemore (1982)] Blakemore, J. S. (1982). *Approximations for Fermi-Dirac integrals, especially the function $F_{1/2}(\eta)$ used to describe electron density in a semiconductor* Solid State Electronics **25**, 1067–1076,
- [Bragg and Kleeman (1904)] Bragg, W. H. and Kleeman, R. (1904). *On the ionization curves of radium* Philos. Mag. **8:48**, 726–738,
- [Bragg and Kleeman (1905)] Bragg, W. H. and Kleeman, R. (1905). *On the α particles of radium, and their loss of range in passing through various atoms and molecules* Philos. Mag. **10:57**, 318–340,
- [Capote *et al* (2009)] Capote, R., Herman, M., Obložinský, P., Young, P. G., Goriely, S., Belgya, T., Ignatyuk, A. V., Koning, A. J., Hilaire, S., Plujko, V. A., Avrigeanu, M., Bersillon, O., Chadwick, M. B., Fukahori, T., Ge, Z., Han, Y., Kailas, S., Kopecky, J., Maslov, V. M., Reffo, G., Sin, M., Soukhovitskii, E. Sh. and Talou, P. (2009). *R1PL - Reference input parameter library for calculations of nuclear reactions and nuclear data evaluations* Nucl. Data Sheets **110** 3107–3214 , Special Issue on Nuclear Reaction Data,
- [Chaudhry and Qadir (2007)] Chaudhry, M. A. and Qadir, A. (2007). *Operator representation of Fermi-Dirac and Bose-Einstein integral functions with applications* Hindawi Publishing Corporation International Journal of Mathematics and Mathematical Sciences article ID 80515, 9 pp.
- [Costin and Garoufalidis (2007)] Costin, O. and Garoufalidis, S. (2007). *Resurgence of the fractional polylogarithms* arXiv:math/0701743v4 [math.CA]
- [Dechargè and Gogny (1980)] Dechargè, J. and Gogny, D. (1980). *Hartree-Fock-Bogolyubov calculations with the D1 effective interaction on spherical nuclei* Phys. Rev. C **21**, 1568–1593,
- [Dingle (1957)] Dingle, R. B. (1957) *The Fermi-Dirac integrals $\mathcal{F}_p(\eta) = (p!)^{-1} \int_0^\infty \varepsilon^p (e^{\varepsilon-\eta} + 1)^{-1} d\varepsilon$* Applied Scientific Research **6** 225–239,
- [Dirac (1984)] Dirac, P. A. M. (1984) *The requirements of fundamental physical theory* Eur. J. Phys. **5** 65–67,
- [Ehrenfest (1927)] Ehrenfest, P. (1927) *Bemerkung über die angenäherte Gültigkeit der klassischen Mechanik innerhalb der Quantenmechanik* Z. Phys. **45** 455–457,
- [Fermi (1934)] Fermi, E. (1934) *Possible production of elements of atomic number higher than 92* Nature **133** 898–899,
- [Fermi (1954)] Fermi, L. (1954) *Atoms in the family: My life with Enrico Fermi*, University of Chicago Press, ISBN 0-88318-524-5
- [Flerov and Petrzhak (1940)] Flerov, G. N. and Petrzhak, K. A. (1940) *Spontaneous fission of*

- uranium* J. Phys. **3** 275–280
- [Geiger and Marsden (1909)] Geiger, H. and Marsden, E. (1909). *On a diffuse reflection of the α -particles* Proc. R. Soc. Lond. A **82**, 495–500,
- [Goldschmidt *et al* (2015)] Goldschmidt, A., Qiu, Z., Shen, C and Heinz, U. (2015). *Collision geometry and flow in uranium + uranium collisions* Phys. Rev. C **92**, 044903,
- [Gomes (1959)] Gomes, L. (1959). *Imaginary part of the optical potential* Phys. Rev. C **116**, 1226–1229,
- [Gonzales and Woods (2018)] Gonzales, R. C. and Woods, R. E. (2018). *Digital image processing. 4th edition* Pearson, Harlow, England
- [Hahn and Straßmann (1939)] Hahn, O. and Straßmann, F. (1939) *Über den Nachweis und das Verhalten der bei der Bestrahlung des Urans mittels Neutronen entstehenden Erdalkalimetalle* Die Naturwissenschaften **27** 11–15,
- [Herrmann (2018)] Herrmann, R. (2018) *Fractional calculus - an introduction for physicists* 3rd ed., World Scientific Publ., Singapore
- [Hilfer (2000)] Hilfer, R. (2000) *Applications of fractional calculus in physics* World Scientific Publ., Singapore
- [Hodgson (1967)] Hodgson, P. E. (1967). *The optical model of the nucleon-nucleus interaction* Annu. Rev. Nucl. Sci. **17**, 1–32,
- [Hofstatter (1956)] Hofstatter, R. (1956). *Electron scattering and nuclear structure* Rev. Mod. Phys. **28**, 214–254,
- [Hossenfelder (2018)] Hossenfelder, S. (2018). *Lost in math: How beauty leads physics astray* Basic Books; Illustrated edition (12 Jun. 2018)
- [Joliot and Curie (1934)] Joliot, F. and Curie, I. (1934). *Artificial production of a new kind of radioelement* Nature **133**, 201–202,
- [Jones (1963)] Jones, P. B. (1963). *The optical model in nuclear and particle physics* Interscience Tracts on Physics and Astronomy, **14**, Wiley and Sons, New York, London
- [Koning and Delaroche (2003)] Koning, A. J. and Delaroche, J-P. (2003). *Local and global nucleon optical models from 1 keV to 200 MeV* Nucl. Phys. **713**, 231–310,
- [Koning *et al* (2014)] Koning, A. J., Rochman, D. and van der Merck, S. C. (2014). *Extension of TALYS to 1 GeV* Nucl. Data Sheets **118**, 187–190,
- [Liouville (1832)] Liouville, J. (1832) *Sur le calcul des différentielles à indices quelconques* J. École Polytechnique **13** 1–162,
- [Mainardi (2010)] Mainardi, F. (2010) *Fractional calculus and waves in linear viscoelasticity: An introduction to mathematical models* World Scientific Publ., Singapore
- [Meitner and Fritsch (1939)] Meitner, L. and Fritsch, O. R. (1939) *Disintegration of uranium by neutrons: A new type of nuclear reaction* Nature **143** 239–240,
- [Mellin (1897)] Mellin, H. (1897) *Über hypergeometrische Reihen höherer Ordnungen* ex Officiina typographica Societatis litterariae fennicae **23**(7) 10pp, Helsingfors, Finland
- [Miller and Ross (1993)] Miller, K. and Ross, B. (1993) *An introduction to fractional calculus and fractional differential equations* Wiley, New York.
- [Millev (1996)] Millev, Y. (1993) *Bose - Einstein integrals and domain morphology in ultrathin ferromagnetic films with perpendicular magnetization* J. Phys. Condensed Matter **8** 3671–3676,
- [Mittag-Leffler (1903)] Mittag-Leffler, M. G. (1903) *Sur la nouvelle fonction $E_\alpha(x)$* Comptes Rendus Acad. Sci. Paris **137** 554–558.
- [Mueller *et al* (2011)] Mueller, J. M. *et al* (2011) *Asymmetry dependence of nucleon correlations in spherical nuclei extracted from a dispersive-optical-model analysis* Phys. Rev. C **83** 064605, 32pp.,
- [NIST (2012)] National Institute of Standards and Technology (NIST) (2012) *Chemistry webBook, NIST standard reference database number 69*
- [Oganessian *et al* (2004)] Oganessian, Yu. Ts. *et al* (2004) *Measurements of cross sections for the fusion-evaporation reactions $Pu-244 (Ca-48, xn) (292-x)114$ and $Cm-245 (Ca-48, xn) (293-x)116$* Phys. Rev. C **69** 054607,
- [Oldham and Spanier (1974)] Oldham, K. B. and Spanier, J. (1974) *The fractional calculus* Academic Press, New York
- [Oppenheimer and Volkoff (1939)] Oppenheimer, J. R. and Volkoff, G. M. (1939) *On massive neutron cores* Phys. Rev. **55** 374–381,
- [Ortigueira (2011)] Ortigueira, M. D. (2011) *Fractional calculus for scientists and engineers* Springer, Berlin, Heidelberg, New York
- [Ostrofsky *et al* (1936)] Ostrofsky, M, Breit, G. and Johnson, D. P. (1936). *The excitation function of lithium under proton bombardment* Phys. Rev. **49**, 22–34,
- [Pauli (1927)] Pauli, W. (1927). *Über Gasentartung und Paramagnetismus* Z. Phys. A **41**, 81–102,

- [Perey and Buck (1962)] Perey, F. and Buck, B. (1962). *A nonlocal potential model for the scattering of neutrons by nuclei* Nucl. Phys. **32**, 353–380,
- [Podlubny (1999)] Podlubny, I. (1999) *Fractional differential equations* Academic Press, New York
- [Rafelski and Müller (1982)] Rafelski, J. and Müller (1982). *Strangeness production in the quark-gluon plasma* Phys. Rev. Lett. **48**, 1066–1069,
- [Rafelski and Müller (1986)] Rafelski, J. and Müller (1986). *Erratum: strangeness production in the quark-gluon plasma* Phys. Rev. Lett. **56**, 2334,
- [Rapaport et al (1986)] Rapaport, J. , Kulkarni, V. and Finlay, R. W. (1979). *A global optical-model analysis of neutron elastic scattering data* Nucl. Phys. **A330**, 15–28,
- [Reinhardt and Greiner (1977)] Reinhardt, J. and Greiner, W. (1977). *Quantum electrodynamics of strong fields* Rep. Prog. Phys. **40**, 219–295,
- [Reinhardt et al (1981)] Reinhardt, J. , Müller, B. and Greiner, W. (1981). *Theory of positron production in heavy-ion collisions* Phys. Rev. A **24**, 103–128,
- [Riemann (1847)] Riemann, B. (1847) *Versuch einer allgemeinen Auffassung der Integration und Differentiation* in: Weber, H. and Dedekind, R. (Eds.) (1892) *Bernhard Riemann's gesammelte mathematische Werke und wissenschaftlicher Nachlass* Teubner, Leipzig, reprinted in *Collected works of Bernhard Riemann* Dover Publications (1953) 353–366
- [Rose and Jones (1984)] Rose, H. J. and Jones, G. A. (1984) *A new kind of natural radioactivity* Nature **307** 245–247,
- [Rutherford (1911)] Rutherford, R. (1911). *The scattering of α and β particles by matter and the structure of the atom* The London, Edinburgh, and Dublin Philosophical Magazine and Journal of Science **21**, LXXIX., 669–688,
- [Rutherford (1919)] Rutherford, R. (1919). *Collision of α particles with light atoms. IV. An anomalous effect in nitrogen* The London, Edinburgh, and Dublin Philosophical Magazine and Journal of Science **37**, LIV., 581–587,
- [Sachdev (1993)] Sachdev, S. (1993). *Polylogarithm identities in a conformal field theory in three dimensions* Phys. Let. B **309** 285–288,
- [Samko et al (1993)] Samko, S. G., Kilbas, A. A. and Marichev, O. I. (1993) *Fractional integrals and derivatives* Translated from the 1987 Russian original, Gordon and Breach, Yverdon
- [Satchler and Love (1979)] Satchler, G. R. and Love, W. G. (1979). *Folding model potentials from realistic interactions for heavy-ion scattering* Phys. Rep. **55** 183–254,
- [Sommerfeld (1928)] Sommerfeld, A. (1928). *Zur Elektronentheorie der Metalle auf Grund der Fermischen Statistik* Z. Phys. A **47**, 1–32,
- [Tao (2022)] Tao, J. (2022). *Zeta annuities, fractional calculus, and polylogarithms* available at SSRN: ssrn.com/abstract=4049283
- [Tarasov (2008)] Tarasov, V. E. (2008). *Fractional vector calculus and fractional Maxwell's equations* Annals of Physics **323**, 2756–2778
- [Tarasov (2016)] Tarasov, V. E. (2016). *Leibniz rule and fractional derivatives of power functions* J. Comput. Nonlinear Dynam., **11**, 031014, 4 pp.
- [Tarasov (2021)] Tarasov, V. E. (2021). *General fractional vector calculus* Mathematics, **9**, 2816
- [Thomson (1904)] Thomson, J. J. (1904). XXIV. *On the structure of the atom: an investigation of the stability and periods of oscillation of a number of corpuscles arranged at equal intervals around the circumference of a circle; with application of the results to the theory of atomic structure* Philosophical Magazine Series 6, **7** **39**, 237–265
- [Tian et al (2015)] Tian, Y., Pang, D. Y. and Ma, Z. Y. (2015). *Systematic nonlocal optical model potential for nucleons* Int. J. Mod. Phys. E, **24** , 1550006
- [Tooper (2021)] Tooper, R. F. (1969). *On the equation of state of a relativistic Fermi-Dirac as at high temperatures* APJ, **156**, 1075–1100
- [Varner et al (1991)] Varner, R. L., Thompson, W. J, McAbee, T. L. Ludwig, E. J. and Clegg, T. B, (1991) *A global nucleon optical model potential* Phys. Rep. **201** 57–119,
- [Walter and Guss (1986)] Walter, R. L and Guss, P. P, (1986) *A global optical model for neutron scattering for $A > 53$ and $10 < E < 80$ MeV* Proc. Int. Conf. on Nuclear Data for Basic and Applied Sciences, Santa Fe, N.M., U.S.A., Gordon and Breach, p.1079
- [Wilson (1946)] Wilson, R. R., (1946) *Radiological use of fast protons* Radiology **47:5** 487–491,
- [Wiman (1905)] Wiman, A. (1905) *Über den Fundamentalsatz in der Theorie der Funktionen $E_a(x)$* Acta Math. **29** 191–201,
- [Wolfram (2022)] Wolfram, S. (2022) *Wolfram Mathematica documentation center*
- [Wolt (2017)] Wolt, P. (2017) *Not even wrong: The failure of string theory and the search for unity in physical law*, Basic Books, NY
- [Wood (1992)] Wood, D. C. (1992). *The computation of polylogarithms*, Technical Report 15-92, Canterbury, UK: University of Kent Computing Laboratory

- [Woods *et al* (1982)] Woods, C. L., Brown, B. A. and Jelley, N. A. (1982). *A comparison of Woods-Saxon and double-folding potentials for lithium scattering from light target nuclei* J. Phys. G.: Nucl. Phys. **8**, 1699–1719,
- [Woods and Saxon (1954)] Woods, R. D. and Saxon, D. S. (1954). *Diffuse surface optical model for nucleon-nuclei scattering* Phys. Rev. **95**, 577–578
- [Xu *et al* (2016)] Xu, C. , Yan, Y. and Shi, Z. (2016). *Euler sums and integrals of polylogarithm functions* J. Num. Th. **165**, 84–108